Master's thesis

NTNU
Norwegian University of Science and Technology
Faculty of Information Technology and Electrical Engineering
Department of Electric Power Engineering

Astrid Sigurdsøn

# Stability Analysis of a New Class of Inner Loops for Voltage Regulation in DC/DC converters

Master's thesis in Energy and Environmental Engineering
Supervisor: Gilbert Bergna-Diaz
June 2023

NTNU
Norwegian University of
Science and Technology

Astrid Sigurdsøn

# Stability Analysis of a New Class of Inner Loops for Voltage Regulation in DC/DC converters

Master's thesis in Energy and Environmental Engineering
Supervisor: Gilbert Bergna-Diaz
June 2023

Norwegian University of Science and Technology
Faculty of Information Technology and Electrical Engineering
Department of Electric Power Engineering

NTNU
Norwegian University of
Science and Technology

## Preface

*As the work conducted in my master's thesis has come to an end, I would like to express my appreciation to my supervisor, Professor Gilbert Bergna-Diaz. Thanks to him I have understood new topics and acquired the necessary knowledge for this master's thesis.*

*I would also like to thank my fellow students at the university for this last year, with special gratitude towards the students at the Corner Office. The engaging discussions, shared laughter, and support provided by them have been essential this last year.*

*And last, but not least, I want to express my gratitude towards family and friends.*

**Abstract**

The production of energy from solar and wind power is anticipated to increase by 35 % in the next seven years. This growth will be facilitated by the incorporation of power electronics technology, which enables the integration of these variable renewable energy sources (RES) into the electrical power grid.

The master's thesis considers the closed-loop stability of a linear DC/DC converter using Lyapunov's method. A port-Hamiltonian (pH) representation is applied for the system equations, and the system controller is inspired by the widely-acknowledged passivity-based Proportional-Integral controller (PI-PBC). However, instead of only using the conventional passive output; i.e., inductor current error signal, the capacitor voltage error signal is also included. The controller was revised building upon the recommendations given in the preliminary work [1]; that is, if the voltage error signal is used as the only input to the PI controller, the system encounters significant stability challenges. Therefore, we propose to utilize the current error signal control in the proportional channel, and the voltage error signal appears in the integral channel of the PI controller.

The proposed PI controller rendered the system globally asymptotically stable (GAS) if a constant leakage term is included in the integral channel next to the system's output voltage error signal. Simulations for this control proposal with a constant leakage were carried out to quantify how much it affects the system's ability to reach its control objectives. Unfortunately, the amount of leakage required created voltage deviations that would not be considered acceptable in practice. Thus, we proceeded to remove the leakage and search for an alternative Lyapunov function to prove stability.

With the aim of proving GAS, a new Lyapunov function candidate (LFC) was proposed without it depending on the presence of a leakage term. The process consisted of populating the Lyapunov function candidate with a constant yet a priori unknown terms relating the physical and control states between them, following the procedure described in [1]. However, it was not possible for us to prove GAS by means of this LFC, as the required constant terms did not seem to exist for the proposed controller.

Nonetheless, because the system and the controller have linear dynamics, the eigenvalues of the closed-loop system could easily be calculated. For a given tuning, the system matrix could be made Hurwitz, and using the Lyapunov equation, a valid Lyapunov function was obtained. With this numerical Lyapunov function, the system was proven GAS. Interestingly, unlike the previous LFC, the new numerical one was *fully* populated. Subsequent to the acquisition of the stability certificate, simulations for the control proposal without the inclusion of the leakage term were carried out.

The populated LFC was utilized to render the system with the inclusion of the leakage term GAS, aiming to reduce the stabilizing leakage term and minimize the required voltage deviations. We showed that increasing the conductance $G$ enhanced the possibility of proving GAS with the populated LFC. Determining the unknown term in the LFC and adjusting the value of $G$, a new condition for the leakage term was established. Simulation results demonstrated a significant decrease in voltage deviations, effectively eliminating them. However, it is worth noting that the higher value of $G$ resulted in spikes in the control signal and increased system losses.

In conclusion, the proposed PI controller gives closed-loop stability in the general, linear DC/DC converter in voltage-control mode directly in the inner-loop. By use of Lyapunov's method, Lyapunov functions exist and render the system GAS.

**Sammendrag**

Energiproduksjonen fra sol- og vindkraft forventes å øke med 35% de neste syv årene. Ved bruk av kraftelektronikkteknologi vil disse fornybare energikildene integreres i det elektriske strømnettet.

Denne masteroppgaven undersøker lukket-sløyfe stabiliteten til en lineær likespenningsomformer ved bruk av Lyapunovs metode. Systemmodellen er representert ved bruk av port-Hamiltonian og systemregulatoren er inspirert av kjente konsept: regulering av passive systemer og en Proporsjonal-Integral (PI) regulator. Kontrollsignalet i en PI-regulator er, med utgangspunkt i regulering av passive systemer, feilsignalet for den passive utgangen i et åpen-sløyfe system, som, i tilfellet for denne omformeren, er spolestrømmen. Denne oppgaven hadde et ønske å bruke feilsignalet til kondensatorspenningen som kontrollsingal i regulatoren, i stedet. I masteroppgavens forarbeid, [1], ble det undersøkt om kondensatorstrømmen sitt feilsignal kunne brukes som eneste inngang til PI-regulatoren. Dette resulterte i stabilitetsproblem. Og dermed ble det vurdert at PI-regulatoren skal ha to forskjellige feilsignal som inngang; spolestrømmen i proporsjonal-kanalen og kondensatorspenningen i integral-kanalen.

Ved bruk av denne PI-regulatoren ble systemet globalt asymptotisk stabilt, gitt inkludering av en konstant lekkasjeverdi i integral-kanalen, i tillegg til feilsignalet for kondensatorstrømmen. Simuleringer for dette kontrollforslaget ble utført for å vurdere hvor mye lekkasjen påvirket systemets evne til å nå sine kontrollmål. Dessverre skapte lekkasjen spenningsavvik som ikke ville bli ansett som akseptable i praksis. Derfor valgte vi å fjerne lekkasjen og lete etter en alternativ Lyapunov-funksjon for å bevise stabilitet.

En ny Lyapunov-funksjon-kandidat ble foreslått med mål om å bevise globalt asymptotisk stabilitet for et system uten inkluderingen av lekkasjen. Lyapunov-funksjonen ble fylt med konstanter som er relevante for de fysiske tilstandene til systemet og noen ukjente som skulle avgjøres i henhold til metoden beskrevet i [1]. Imidlertid var det ikke mulig for oss å bevise global asymptotisk stabilitet ved hjelp av denne Lyapunov-funksjon-kandidaten, da den nødvendige konstanten ikke var mulig å definere.

Ettersom systemmodellen og regulatoren har lineær dynamikk, ble egenverdiene til systemet beregnet. Og for en gitt innstilling av regulatorverdiene, ble egenverdiene negative og systemmatrisen Hurwitz. Videre, ble Lyapunov-ligningen brukt for å beregne en gyldig Lyapunov-funksjon. For denne numeriske Lyapunv-funksjonen ble systemet vist globalt asymptotisk stabilt. En interessant observasjon for denne numeriske Lyapunov-funksjonen, sammenlignet med den foreslåtte, er at den var fullstendig fullt opp av elementer. Etter å ha oppnådd stabilitetsgaranti ble simuleringer utført for dette systemet.

Den foreslåtte Lyapunov-funksjon-kandidaten ble videre brukt for å vise global asymptotisk stabilitet i systemet som inkluderte lekkasjen. Med mål om å redusere lekkasjen som var nødvendig for et stabilt system og dermed redusere også spenningsavvikene. Vi viste at økning i konduktansen $G$ økte muligheten for et stabilt system for den foreslåtte Lyapunov-funksjon-kandidaten. Ved å bestemme den ukjente konstanten i funksjonen og justere opp verdien av konduktansen, ble det satt en ny betingelse for lekkasjekonstanten. Simuleringer viste en betydelig reduksjon i spenningsavvikene. Det er imidlertid verdt å merke seg at den høyere verdien av $G$ resulterte i ekstremt høye verdier i kanalen for kontrollsignalet og økt effekttap i systemet.

Konklusjonen for denne masteroppgaven er at den foreslåtte PI-regulatoren gir lukket-sløyfe stabilitet i den lineære likespenningsomformer, i spenningskontrollmodus, direkte i den indre løkken. Ved bruk av Lyapunovs metode eksisterer det Lyapunov-funksjoner og systemet er globalt asymptotisk stabilt.

# Contents

# List of Figures

# List of Tables

# Abbreviations

| | |
|---|---|
| **AC** | Alternating-current |
| **DC** | Direct-current |
| **EU** | European Union |
| **GAS** | Globally Asymptotically Stable |
| **IEA** | International Energy Agency |
| **KCL** | Kirchhoff's Current Law |
| **KVL** | Kirchhoff's Voltage Law |
| **LFC** | Lyapunov Function Candidate |
| **PBC** | Passivity Based Controller |
| **pH** | port-Hamiltonian |
| **PI** | Proporsjonal-Integral |
| **PI** | Proportional Integral |
| **PV** | Photovoltaics |
| **RES** | Renewable Energy Source |
| **RLC** | Resistor Inductor Capacitor |

# Chapter 1

# Introduction

*This introductory chapter presents the general framework for the master's thesis. As a starting point, the increasing need for RES in power production is explained and put into context why it is expected to have continuous growth in the following years. The objective and the methodology of the thesis are presented, and the necessary simplifications of the system are explained. Lastly, the structure of the master's thesis is presented in a chapter overview. and shows the chronological work order.*

## 1.1 General Introduction

According to the International Energy Agency (IEA), global electricity production from renewable technologies was 28% in 2021, and this share is expected to increase in the coming years. The projected growth says today's production from RES is 32% [2].

The Paris Agreement, made on 12 December 2015 and executed since 4 November 2016, set a goal to limit global warming to well below 2° and pursue efforts to limit the temperature increase to 1.5° [3]. This agreement has been adopted by more than 190 Parties, including the European Union (EU) and its member countries. The EU has set a goal of *"cutting net greenhouse gas house emissions by at least 55% by 2030"* and *"becoming a climate-neutral continent by 2050"* [4] to act by the Paris Agreement. The goal is broken down into targets for each decade, and the next target is to reach 42.5% renewable energy production by 2030 [4]. The share of renewable energy production was 22% in 2021 in the EU, and if they want to achieve the target for 2030, the share has to be increased by 2.4% each year, triple the historical rate [5]. In 2021, the expansion of wind and solar photovoltaic (PV) power generation made the most influential contribution to the increase of RES in the EU. This growth resulted in RES accounting for 37.6% of all electricity generated in the power sector [2].

Per the Paris Agreement, global electricity production from renewable technologies has to reach 90% by 2050 [6]. Reaching this goal means a substantial upscale in RES in the following decades, most of which will occur in solar and wind power production. Today, these technologies have an electrical production share of 7% globally, which has to increase to 42% in 2030 and then 63% in 2050, respectively [6]. These variable RES need a flexible power system that can operate under changing conditions in terms of production and demand peaks due to fluctuating energy supply.

The integration of variable RES using power converter technology, e.g., wind and PV, has led to the replacement of conventional power production, e.g., hydropower utilizing generators, in the power system. Conventional power production has been the fundament for stability in power systems providing inertia and meeting energy-supply demand. By exchanging this steady connection of energy with a fluctuating connection of energy from multiple variable RES, stability problems, such as reduced system strength, synchronous inertia, and black start capability, have risen [7], [8]. These challenges can also arise from devices not related to power production, e.g., energy

storage and charging of electric vehicles, which are connected to the grid through power converter technology [9].

RES are connected to the main grid through power converters. An important role of power converters, specifically DC/DC converters, is to manage the level of DC voltage. Typically by coupling the voltage levels for a RES to a DC/AC inverter [9]. PI-PBC are popularly used in power converter applications, such as DC/DC converters [10] [11].

## 1.2 Objectives and Methodology

The master's thesis investigates the stability of a general, linear DC/DC converter in voltage-control mode *directly in the inner-loop*, thus avoiding any traditional time-scale separation assumptions. More precisely, we propose to utilize a PI controller which uses the inductor current error in the proportional and the capacitor voltage error in the integral channels.

The inductor current turns out to be the passive output of the incremental model of linear DC/DC converters, making it the conventional choice for the error signal using PI-PBC control - albeit operating in current-control mode. By contrast, in [1], we showed that a PI around the capacitor voltage error signal did not render the closed-loop system stable; or, more precisely, by using the capacitor voltage error signal in both the proportional and integral channels of the PI controller. This observation motivated us to reach a compromise between both cases: a) standard PI current control with stability guarantees and b) a PI around the voltage error signal. Thus, a different control scheme is proposed.

This thesis aims to obtain a closed-loop stability certificate, specifically, a Lyapunov function, using the new control scheme. A pH representation is used as a modeling starting point and is applied to the circuit's system, such that its capabilities in energy-storing, -preserving, and -dissipating are highlighted. The model of the circuit's system is shifted to an incremental form to ensure the operating point of interest, a non-zero equilibrium point. Subsequently, Lyapunov's method is used to analyze the system's stability, which can be applied to systems with both linear and non-linear dynamics. Lastly, a simulation model of the system is developed in MATLAB Simulink.

## 1.3 Limitation of Scope

As mentioned previously, the converter circuit model is simplified to have linear dynamics instead of more realistic non-linear ones. This simplification is a useful starting point to gain insight, which could then be extended to the non-linear converter in future works. It is worth recalling that if the system was considered non-linear, it would be more representative as the switching properties of a power converter would be included. The control theory applied is valid for both linear and non-linear cases, and it is possible to apply the results from the analysis to the non-linear case in future works.

The DC/DC converter is represented by a general Resistor-Inductor-Capacitor (RLC) circuit. The master's thesis aims to give general results that apply to DC/DC converters without removing specifications related to a particular converter. And the converter is considered a standalone, with only its input-output characteristics and no interconnection with other components such as RES or another converter. This simplification limits the stability certificate to a single unit, and in the future work section, it is recommended to investigate its potential scalability features.

The main objective of this thesis is to obtain a stability certificate for the system. The focus is on achieving a mathematical proof of stability, which is accomplished through the application of Lyapunov's method. It is important to note that the simulation results, which illustrate the system's dynamics, are not essential for obtaining the stability certificates. They are provided as supplementary information, enhancing the understanding of the system's behavior, but not as a requirement for the stability certificates themselves.

## 1.4 Thesis Structure

The outline of the master's thesis is divided into seven chapters. The first three chapters, including this introduction chapter, cover the introductory framework and knowledge for the thesis' objective. And the last four chapters explore solutions to the closed-loop stability problem for the proposed PI controller and present the conclusion and the possibilities for future works.

Chapter 2, *Theory*, is a continuation of the theory section in the specializations project, obtained from section 2 in [1]. Sections 2.6 and 2.7 were added to the master's thesis work. Section 2.6 was absent from the project but necessary for some of the calculations, and section 2.7 was only relevant for the work conducted in the master's thesis.

Chapter 3, *Preliminaries*, summarizes the preliminary work associated with this master's thesis conducted during the fall semester of 2022 in the specialization project [1].

Chapter 4, *Leakage in the Controller*, contains the system's parameters and simulations for the system model with the inclusion of a leakage term.

Chapter 5, *Populating the LFC*, finishes the calculations for the populated LFC and introduces the solution with a numerical Lyapunov function, and contains simulations for the system model without the inclusion of a leakage term.

Chapter 6, *Leakage in the Controller and the Populated LFC Combined*, uses the populated LFC to render the system, with inclusion for leakage, GAS. Following this, a new stabilizing condition for the leakage term is obtained. In simulations, the voltage deviations required by the leakage term are considered.

Chapter 7, *Concusion and Future Works*, summarizes the finding of this master's thesis and presents the possibilities for future work.

Lastly, the appendices to this master's thesis include calculations and proofs from the specialization project that were used as support for the calculations done in the thesis. In addition to the supporting material, the concept of droop control is presented.

# Chapter 2

# Theory

This theory chapter is obtained from section 2 in the specialization project [1] except for sections 2.6 and 2.7, which were included as a part of the work conducted in the master's thesis.

## 2.1 Nonlinear Systems

A common form to represent a general time-invariant nonlinear system is given in equation (2.1.1).

$$\dot{x} = f(x) + g(x)u, \quad y = h(x) \tag{2.1.1}$$

Nonlinear systems are more complex than linear systems due to the possibility of multiple or no equilibrium points. The stability properties of nonlinear systems can therefore be more challenging to determine. Equilibrium points for a system are found through steady-state analysis by setting the time derivative of the state variables equal to zero $\dot{x} = 0$. The real solutions to this equation correspond to the equilibrium points of the system. If the system only has the origin as an equilibrium point, it is possible to analyze the stability using Lyapunov's direct method.

In (2.1.1), the variables $u$ and $y$ represent the input and output. The input $u$ is a function of the system's state, and the closed-loop system is obtained when this feedback information, $u = \gamma(x)$, is provided to the system.

## 2.2 Lyapunov's Method

Lyapunov's method is used for the stability analysis of both linear and nonlinear systems. There are two main approaches to applying Lyapunov's method: the direct method and the indirect method.

The indirect method is the approach when a nonlinear system has more than one equilibrium point. However, this method is based on linearizing the nonlinear system and can only provide local asymptotic stability at each equilibrium point. The direct method can be used to analyze systems with a single equilibrium point and determine whether the equilibrium point is stable, asymptotically stable, or globally asymptotically stable.

$\mathcal{V}(x)$ is a *Lyapunov function* for the origin if and only if three conditions hold in the domain $\mathbb{D}$. The following conditions for a Lyapunov function are given in *Theorem 4.1* in Khalil's Nonlinear Systems [12].

i) $\mathcal{V}$ is $C^1$

$$\begin{aligned} &\text{ii)} \quad \mathcal{V}(0) = 0 \\ &\qquad \mathcal{V}(x) > 0 \quad \forall x \neq 0 \in \mathbb{D} \\ &\text{iii)} \quad \dot{\mathcal{V}}(0) = 0 \\ &\qquad \dot{\mathcal{V}}(x) \leq 0 \quad \forall x \neq 0 \in \mathbb{D} \end{aligned}$$

A function $\mathcal{V}(x)$ must satisfy three conditions to serve as a Lyapunov function. The first condition is that $\mathcal{V}(x)$ must be continuously differentiable $C^1$. The second condition is that $\mathcal{V}(x)$ must be *positive definite* within the domain $\mathbb{D}$ and have a minimum value at the origin. The third condition is that the time derivative of $\mathcal{V}(x)$, denoted $\dot{\mathcal{V}}(x)$, must be *negative semi-definite*. Negative semi-definite ensures stability within the domain. If, in addition, $\dot{\mathcal{V}}(x) < 0$, then $\dot{\mathcal{V}}(x)$ is *negative definite*, which indicates asymptotic stability as the trajectory of the system's solutions, not only approach the origin but converge to it. If $\dot{\mathcal{V}}$ is negative definite, then $\mathcal{V}(x)$ is a strict Lyapunov function for $x = 0$.

$\dot{\mathcal{V}}(x)$ is dependent on the system's equations since it is the derivative along the trajectories of the system, and $\dot{\mathcal{V}}(x)$ will be different for different systems. All three conditions need to be satisfied by the chosen function $V(x)$ to prove the stability of the system.

To ensure global asymptotic stability, a fourth condition is included. This condition is stated in *Theorem 4.2* in Khalil's Nonlinear Systems [12].

$$\text{iv)} \quad \|x\| \to \infty \Rightarrow \mathcal{V}(x) \to \infty$$

The final condition for a Lyapunov function is that the norm of the states $x$ must be radially unbounded. If this condition is satisfied, the Lyapunov function will also be radially unbounded. The origin will be GAS if the Lyapunov function satisfies all four conditions.

## 2.3 Passive Systems

A definition of passive systems is given by Loría and Nijmeijer in [13];

> "*From an energetic viewpoint we can define a passive system as a system which cannot store more energy than is supplied by some 'source', with the difference between stored energy and supplied energy, begin the dissipated energy.*"

In an electrical system, the energy is the power inflow, and this can be expressed as the product of the input voltage and the output current. The energy stored in a system is determined by a storage function, with a common application being a Lyapunov function. A passive dynamical system is mathematically represented in (2.3.1).

$$u^\top y \geq \dot{\mathcal{V}} \tag{2.3.1}$$

Equation (2.3.1) represents an open-loop system with an undefined input $u$ and the storage function $\mathcal{V}(x)$. According to the definition above, the dissipated energy in the system will be $\dot{V} - u^\top y$. *Lemma 6.6* in Khalil's *Nonlinear systems* [12] states that if the passivity in (2.3.1) holds and if the input to the system $u = 0$, then the system is stable. If the dissipation energy of the system is included as well, then (2.3.2) is stable.

$$\dot{\mathcal{V}} \leq \text{dissipated energy} \tag{2.3.2}$$

## 2.4 Port-Hamiltonian

A port-modeling of a system represents its input and output characteristics in terms of the flow of energy through the system. pH modeling combines port modeling with a Hamiltonian function, which describes the total energy stored in the system and is recognized as a natural starting point for the control of nonlinear systems. Due in part to its ability to incorporate energy considerations and to represent interconnections between systems.

Power electronics systems can be described by pH modeling. The general representation of a power electronics converter in pH is given as in (2.4.1) [11].

$$\dot{x} = \left( \mathcal{J}_o + \sum_{i=1}^{m} \mathcal{J}_i u_i - \mathcal{R} \right) \nabla \mathcal{H}(x) + \left( G_o + \sum_{i_1}^{m} G_i u_i \right) E \tag{2.4.1}$$

As stated in the introduction, the switching properties of the converter are neglected. The relevant representation for the power converter for this project is given in (2.4.2).

$$\dot{x} = (\mathcal{J}_0 - \mathcal{R}) \nabla \mathcal{H}(x) + \left( G_o + \sum_{i_1}^{m} G_i u_i \right) E \tag{2.4.2}$$

The state vector of the converter is given as $x \in \mathbb{R}^n$, the interconnection matrix $\mathcal{J}_o$ is skew-symmetric, the dissipation matrix $\mathcal{R} = \mathcal{R}^\top \geq 0$, and in the last term $G_o E$, $E$ is the external sources vector.

The gradient of the Hamiltonian function, $\nabla \mathcal{H}(x)$, describes the total energy stored in the system. The Hamiltonian of the system is given by (2.4.3) [14].

$$\mathcal{H}(x) := \frac{1}{2} x^\top Q x \quad \Rightarrow \quad \nabla \mathcal{H}(x) = Qx, \quad Q = Q^\top > 0 \tag{2.4.3}$$

the symmetric matrix $Q$ contains information about the energy-storing components, e.g., inductors and capacitors of the system.

## 2.5 Relevant Properties of Square Matrices

Given a trivial square matrix $\mathbf{M}_{n \times n}$ and its transpose $\mathbf{M}^\top_{n \times n}$.

Any matrix $\mathbf{M}$ is the sum of a symmetric matrix and a skew-symmetric matrix; $\mathbf{M} = \mathbf{M}_{sym} + \mathbf{M}_{skew}$ [15]. The symmetric and the skew-symmetric parts of $\mathbf{M}$ are given in (2.5.1) and (2.5.2), respectively.

$$\mathbf{M}_{sym} = \frac{1}{2}(\mathbf{M} + \mathbf{M}^\top) \tag{2.5.1}$$

$$\mathbf{M}_{skew} = \frac{1}{2}(\mathbf{M} - \mathbf{M}^\top) \tag{2.5.2}$$

Positive definiteness is an important property when conducting Lyapunov's direct method. If the symmetric part of $\mathbf{M}$, $\mathbf{M}_{sym}$, is positive definite, then $\mathbf{M}$ is positive definite [15].

$\mathbf{M}$ is a symmetric matrix if $\mathbf{M} = \mathbf{M}^\top$, and if $\mathbf{M}^\top = -\mathbf{M}$ then the matrix is skew-symmetric. If a skew-symmetric matrix $\mathbf{M}$ is multiplied by a symmetric vector $\mathbf{N}$ on both sides, the final product is zero.

$$\mathbf{N}^\top \mathbf{M} \mathbf{N} = \frac{1}{2} \mathbf{N}^\top \mathbf{M} \mathbf{N} - \frac{1}{2} \mathbf{N} \mathbf{M}^\top \mathbf{N}^\top = \frac{1}{2} \mathbf{N}^\top \mathbf{M} \mathbf{N} - \frac{1}{2} \mathbf{N}^\top \mathbf{M} \mathbf{N} = 0 \tag{2.5.3}$$

## 2.6 Schur Complement

Given a symmetric matrix $\mathbf{M}$:

$$\mathbf{M} = \begin{bmatrix} A & B \\ B^\top & C \end{bmatrix} \tag{2.6.1}$$

To determine if matrix $\mathbf{M}$ is positive definite, the Schur complement can be calculated. In addition to $\mathbf{M}$ being symmetric, $A > 0$ and has to be invertible. If the calculated Schur complement is larger than zero, then the matrix is positive definite [16]. The Schur complement calculated for matrix $\mathbf{M}$ is given as:

$$C - B^\top A^{-1} B > 0 \tag{2.6.2}$$

## 2.7 Lyapunov Equation

The system matrix $A$, of a system with linear dynamics is Hurwitz if all the eigenvalues are negative. The Lyapunov equation can be applied, if $A$ is Hurwitz, to find a positive definite symmetric matrix $\mathcal{P}$ for any given positive definite symmetric matrix $\mathcal{Q}$ [12] :

$$\mathcal{P}A + A^\top \mathcal{P} = -\mathcal{Q} \tag{2.7.1}$$

The Lyapunov function $\mathcal{V}(x)$ is defined as the positive definite matrices $\mathcal{P}$ and $\mathcal{Q}$:

$$\mathcal{V}(x) = x^\top \mathcal{P} x \quad \text{and} \quad \dot{\mathcal{V}}(x) = -x^\top \mathcal{Q} x$$

## 2.8 PI-controller and PBC

### 2.8.1 PI-controller

A PI controller is a feedback control regulating a system's output. The input of a PI controller is the error between a signal and a reference signal, and the output is a correction term applied to the system to reduce the error. The general form of a PI controller is given by equation (2.8.1), where $e(t)$ is the input error signal and $u(t)$ is the output correction signal.

$$u(t) = K_P e_P(t) + K_I \int e_I(t) dt \tag{2.8.1}$$

$K_P$ and $K_I$ are positive gain constants that are tuned according to the characteristics of the system. Equation (2.8.1) can also be written in negative form, as shown in equation (2.8.2).

$$u(t) = -K_P y_P(t) - K_I \int y_I(t) dt \tag{2.8.2}$$

The controller is designed by defining $y(t) := e(t)$.

Equation (2.8.2) operates in current-control mode by setting $e = i - i^{\text{ref}}$ for the integral channel, or in voltage-control mode for $e = v - v^{\text{ref}}$.

### 2.8.2 PBC

A passivity-based controller (PBC) is a control based on the passivity properties of open-loop energy-storing systems, which aims to design a controller that ensures that the closed-loop system is stable [13]. The stability property is proved using Lyapunov; therefore, the system has to be stable at the origin. The method uses the storage function of a passive system as the Lyapunov function and designs a controller which renders the system asymptotically stable [12] [14].

# Chapter 3

# Preliminearies

This chapter summarizes the work conducted in the preliminary specialization project in the fall of 2022 [1] as this was not published. The chapter consists of system modeling, the stability analysis when a leakage term was included in the controller, and the initial part of designing an LFC by populating it with unknown terms. The material in this chapter is essential for the work conducted in the master's thesis. This chapter's outline is the same as the project's outline in [1], but the material is rewritten and condensed. Some proofs are not included in the master's thesis but are referred to in the project or in the appendix.

## 3.1 System Modeling

A general RLC circuit is used to represent a DC/DC converter in figure 3.1.

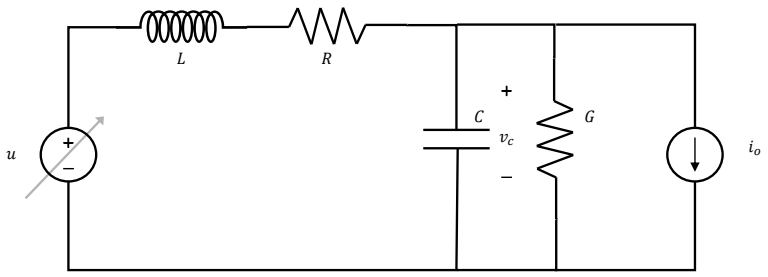


Figure 3.1: RLC circuit

### 3.1.1 Modeling of the System Equations

Differential equations of the system, the system equations, are derived using Kirchhoff's current (KCL) and voltage laws (KVL):

$$\begin{bmatrix} \dot{i}_L \\ \dot{v}_C \end{bmatrix} = \begin{bmatrix} \frac{-R}{L} & \frac{-1}{C} \\ \frac{1}{L} & \frac{-G}{C} \end{bmatrix} \begin{bmatrix} i_L \\ v_C \end{bmatrix} + \begin{bmatrix} \frac{1}{L} \\ 0 \end{bmatrix} u + \begin{bmatrix} 0 \\ \frac{-1}{C} \end{bmatrix} i_o \tag{3.1.1}$$

and the system's output is given as the inductor current $i_L$.

The inductor and the capacitor are the passive elements of the circuit, and make it possible to consider the system as passive. Due to this and to observe the energy-conserving capabilities in the

circuit, a pH representation was utilized. The states in the pH form are the flux in the inductor, $\Phi_L$, and the charge of the capacitor, $q_C$.

The pH representation is given in (3.1.2).

$$\begin{bmatrix} \dot{\Phi}_L \\ \dot{q}_C \end{bmatrix} = \begin{bmatrix} -R & -1 \\ 1 & -G \end{bmatrix} \begin{bmatrix} i_L \\ v_C \end{bmatrix} + \begin{bmatrix} 1 \\ 0 \end{bmatrix} u + \begin{bmatrix} 0 \\ -1 \end{bmatrix} i_o \tag{3.1.2}$$

The output of the system is not changed by the new representation and remains the inductor current $i_L$. The specific matrix definitions for the system are given in appendix A.1.

The general representation of the circuit is given as:

$$\dot{x} = (\mathcal{J}_o - \mathcal{R})\nabla\mathcal{H}(x) + gu + E_o \tag{3.1.3}$$

**The Incremental Model**

If the operating point in a DC/DC converter is at the origin, the system's setpoints are equal to zero, and a converter is turned off. Conducting a stability analysis for a system, in that case, would be redundant as it is apparent that a turned-off system is stable.

Instead, the system's desired operating points are at non-zero equilibrium points, and, therefore, the model of the system is shifted to an incremental model. The system was shifted for the wanted operating points, $x$, and their respective equilibrium points, $\bar{x}$ [17]. The incremental model is given as $\tilde{x} := x - \bar{x}$.

The general system representation is given in the incremental form:

$$\dot{\tilde{x}} = \underbrace{(\mathcal{J}_0 - \mathcal{R})}_{\mathcal{F}_o} \nabla\mathcal{H}(\tilde{x}) + g\tilde{u} \tag{3.1.4}$$

The system matrix, $\mathcal{F}_o$, and the controller matrix, $g$, remain the same. Whereas the term $E_o$ was eliminated. The final system representation is given in (3.1.5).

$$\begin{bmatrix} \dot{\tilde{\Phi}}_L \\ \dot{\tilde{q}}_C \end{bmatrix} = \begin{bmatrix} -R & -1 \\ 1 & -G \end{bmatrix} \begin{bmatrix} \tilde{i}_L \\ \tilde{v}_C \end{bmatrix} + g\tilde{u} \tag{3.1.5}$$

The dynamics of the model and the incremental model are equivalent. The proof of this is given in appendix A.2.

### 3.1.2 Modeling of the Controller

The passive output of the incremental model of this system is given in (3.2.2) and is the inductor current. The passive output of the incremental system is the same as the passive output of the original system because the systems are equivalent, i.e., the system model has inductor current as passive output.

In the specialization project [1], the system was considered to operate in voltage-control mode by using the capacitor voltage error as input to the proportional and integral channels in the PI controller. This type of control had no guarantees of stability as it was not designed from the system's passive output. After a stability analysis was conducted, the eigenvalues of this system had an indeterminate sign, as seen in appendix B, and, therefore, the control was not considered advantageous for stability.

The proposed PI controller has the inductor current error as input to the proportional channel and the capacitor voltage error as input to the integrator channel. The system model operates in voltage-control mode as well as considering the passive output for stability purposes.

The controller is given as in (3.1.6).

$$u = -K_P y + K_I x_c \tag{3.1.6}$$

with $y = i_L - i_L^*$. The use of $i_L^*$ instead of $i_L^{\text{ref}}$ is explained in appendix C.2.

The integral channel has the capacitor voltage as input. Therefore, the controller state $\dot{x}_c$ is defined as the negative signal for capacitor voltage error:

$$\dot{x}_c = -y_2 \tag{3.1.7}$$

with $y_2 = v_C - v_C^{\text{ref}}$.

The controller in incremental form is given in (3.1.8). The incremental model of the controller is derived in appendix A.2.

$$\tilde{u} = -K_P \tilde{y} + K_I \tilde{x}_c \tag{3.1.8}$$

## 3.2 Stability Analysis

The system is passive, and its passive output is the inductor current. This was verified by the use of Lyapunov's method in the project [1].

### 3.2.1 Open-Loop Stability

The Hamiltonian $\mathcal{H}(\tilde{x})$ is used as a Lyapunov function for the system:

$$\mathcal{V}_1(\tilde{x}) = \mathcal{H}(\tilde{x}) = \frac{1}{2}\tilde{x}^\top Q \tilde{x} \tag{3.2.1}$$

The time derivative $\dot{\mathcal{V}}_1$ is calculated. By use of skew-symmetric and positive definite properties, the expression is simplified.

$$\begin{aligned}\dot{\mathcal{V}}_1(\tilde{x}) &= \underbrace{\nabla^\top \mathcal{H}(\tilde{x}) \mathcal{J}_o \nabla \mathcal{H}(\tilde{x})}_{0} - \underbrace{\nabla^\top \mathcal{H}(\tilde{x}) \mathcal{R} \nabla \mathcal{H}(\tilde{x})}_{\geq 0} + \nabla^\top \mathcal{H}(\tilde{x}) g \tilde{u} \\ &\leq \nabla^\top \mathcal{H}(\tilde{x}) g = \tilde{x}^\top Q g \tilde{u} = \tilde{y}^\top \tilde{u}\end{aligned}$$

The incremental model has a passive output $\tilde{y}$:

$$\dot{\mathcal{V}}_1(\tilde{x}) \leq \tilde{y}^\top \tilde{u} \tag{3.2.2}$$

which is identified as the inductor current.

The system model and the incremental model are equivalent; therefore, the system model's passive output is also the inductor current.

### 3.2.2 Closed-Loop Stability

To analyze the stability of the closed-loop system, the controller (3.1.8) is given as input to system (3.1.5). Additionally, the state space is extended to include the controller state, $\dot{\tilde{x}}_c$.

The proposed LFC for the whole state space system:

$$\mathcal{V}_2(\tilde{x}, \tilde{x}_c) = \frac{1}{2}\tilde{x}^\top Q \tilde{x} + \frac{1}{2}\tilde{x}_c^\top K_I \tilde{x}_c \tag{3.2.3}$$

Lyapunov's method was applied for the system using (3.2.3) in [1]. However, it was not possible to prove $\dot{\mathcal{V}}_2$ negative definite using (3.1.8) as the controller.

In an attempt to obtain a closed-loop stability certificate, i.e., a Lyapunov function, two different methods were considered. The first method was introducing a leakage term in the controller. And the second method was populating the LFC with unknown terms, which will be determined to ensure the stability of the system.

### Leakage in the Controller

For the case of leakage in the controller, a constant leakage $D$ is included. The new state space system is given in (3.2.4).

$$\begin{cases} \dot{\tilde{x}} = (\mathcal{J}_o - \mathcal{R})Q\tilde{x} + g\tilde{u} \\ \dot{\tilde{x}}_c = -\hat{g}^\top Q\tilde{x} - DK_I\tilde{x}_c \end{cases} \tag{3.2.4}$$

This system uses the same LFC (3.2.3), $\mathcal{V}_2$. But with a new system due to the controller including leakage, the time derivative $\dot{\mathcal{V}}_2$ will be different.

$$\begin{aligned}
\dot{\mathcal{V}}_2 &= \nabla\mathcal{V}_2^\top(\tilde{x}) \cdot \dot{\tilde{x}} + \nabla\mathcal{V}_2^\top(\tilde{x}_c) \cdot \dot{\tilde{x}}_c \\
&= \tilde{x}^\top Q(\mathcal{J}_o - \mathcal{R})Q\tilde{x} + \tilde{x}^\top Qg(-K_P\tilde{y} + K_I\tilde{x}_c) - \tilde{x}_c^\top K_I\hat{g}^\top Q\tilde{x} - \tilde{x}_c^\top K_I D K_I\tilde{x}_c \\
&= -\tilde{x}^\top Q\mathcal{R}Q\tilde{x} - \tilde{x}^\top QgK_Pg^\top Q\tilde{x} + \tilde{x}^\top QgK_I\tilde{x}_c - \tilde{x}_c^\top K_I\hat{g}^\top Q\tilde{x} - \tilde{x}_c^\top K_I D K_I\tilde{x}_c \\
&= -\tilde{x}^\top Q\mathcal{R}Q\tilde{x} - \tilde{x}^\top Q\bar{K}_PQ\tilde{x} + \frac{1}{2}(\tilde{x}^\top QgK_I\tilde{x}_c + \tilde{x}_c^\top K_Ig^\top Q\tilde{x}) - \frac{1}{2}(\tilde{x}_c^\top K_I\hat{g}^\top Q\tilde{x} - \tilde{x}^\top Q\hat{g}K_I\tilde{x}_c) \\
&\quad - \tilde{x}_c^\top K_I D K_I\tilde{x}_c \\
&= -\begin{bmatrix}\tilde{x}^\top Q & \tilde{x}_c^\top K_I\end{bmatrix}\begin{bmatrix}\mathcal{R} + \bar{K}_P & \frac{1}{2}(\hat{g} - g) \\ \frac{1}{2}(\hat{g} - g)^\top & D\end{bmatrix}\begin{bmatrix}Q\tilde{x} \\ K_I\tilde{x}_c\end{bmatrix}
\end{aligned}$$

To condense the expression for $\dot{\mathcal{V}}_2$, $\bar{K}_P := gK_PC^\top$ is used.

Further, to determine stability, the Schur complement of $\dot{\mathcal{V}}_2$ was calculated. $\mathcal{R} + \bar{K}_P$ is invertible as it is a diagonal matrix with positive constants, and the matrix of $\dot{\mathcal{V}}_2$ is symmetric. The Schur complement was calculated directly.

$$D - \frac{1}{4}(\hat{g} - g)^\top(\mathcal{R} + \bar{K}_P)^{-1}(\hat{g} - g) > 0$$

From the calculated Schur complement, a condition for $\dot{\mathcal{V}}_2$ was obtained. If $D > \frac{1}{4}\left(\frac{1}{R+K_P} + \frac{1}{G}\right)$, then $\dot{\mathcal{V}}_2$ is negative definite.

$\mathcal{V}_2$ is positive definite, and its time derivative, with this system model, is negative definite. Therefore, $\mathcal{V}_2$ is a Lyapunov function for this system model as it renders the system GAS. And a stability certificate was obtained for the system using $\mathcal{V}_2$ and a leakage condition for the system, $D > \frac{1}{4}\left(\frac{1}{R+K_P} + \frac{1}{G}\right)$.

The amount of required leakage in the output voltage is calculated from $D > \frac{1}{4}\left(\frac{1}{R+K_P} + \frac{1}{G}\right)$. The value of $D$ results in a deviation between the system's voltage output and its reference. Without knowing the parameters for the system and a simulation model, the exact value of $D$ and the required voltage deviations will subsequently be calculated during the work conducted in the master's thesis. However, in [1] it was assumed that this leakage was substantial enough that it would not be accepted in practice.

Due to the magnitude of the deviations in the output value with the inclusion of a leakage term, it was decided to remove the leakage term from the system's controller. Therefore, it was necessary to find another LFC to prove GAS for the system with the inclusion of leakage.

### Populating the LFC

Instead of introducing a leakage term in the controller's integral channel, a new LFC was required. A possible way to obtain stability is by populating the terms of the LFC with unknown values, then obtaining the time-derivative and choosing the unknowns such that the resulting expression is negative definite.

A typical way to design LFCs is by using quadratic functions to ensure they are positive definite and $C^1$. And the LFC has to depend on the whole state space of the system model.

$$\mathcal{V}_3(\tilde{x}, \tilde{x}_c) = \begin{bmatrix} \tilde{x}^\top & \tilde{x}_c^\top \end{bmatrix} \mathbf{C}_{2\times 2} \begin{bmatrix} \tilde{x} \\ \tilde{x}_c \end{bmatrix}$$

The unknown factor is a matrix, which is set as $\mathbf{C}_{2\times 2}$, and the elements of the matrix have to be populated. To fulfill the first Lyapunov condition, $\mathbf{C}_{2\times 2} = \mathbf{C}_{2\times 2}^\top > 0$, and for the time-derivative of $\mathcal{V}_3$ to maintain the passivity property, it is necessary to include the elements $Q$ and $K_I$ in $\mathbf{C}_{2\times 2}$. Further, to populate the matrix, new elements are introduced: a small scalar $\varepsilon > 0$ and a vector $\mathbf{H}_{2\times 1}$.

$$\mathcal{V}_3(\tilde{x}, \tilde{x}_c) := \frac{1}{2} \begin{bmatrix} \tilde{x}^\top & \tilde{x}_c^\top \end{bmatrix} \underbrace{\begin{bmatrix} Q & -\varepsilon\mathbf{H} \\ -\varepsilon\mathbf{H}^\top & K_I \end{bmatrix}}_{\mathbf{C}_{2\times 2}} \begin{bmatrix} \tilde{x} \\ \tilde{x}_c \end{bmatrix} \tag{3.2.5}$$

$\mathcal{V}_3$ is quadratic, symmetric, and positive definite. The LFC is given in equation form to find the time derivative:

$$\mathcal{V}_3(\tilde{x}, \tilde{x}_c) = \frac{1}{2}\tilde{x}^\top Q\tilde{x} + \frac{1}{2}\tilde{x}_c^\top K_I\tilde{x}_c - \varepsilon\tilde{x}^\top\mathbf{H}\tilde{x}_c \tag{3.2.6}$$

Both $Q$ and $K_I$ are essential in the off-diagonal terms. Therefore, $\mathbf{H} := QgK_I$. $\mathcal{V}_3$ is then:

$$\mathcal{V}_3(\tilde{x}, \tilde{x}_c) = \frac{1}{2}\tilde{x}^\top Q\tilde{x} + \frac{1}{2}\tilde{x}_c^\top K_I\tilde{x}_c - \varepsilon\tilde{x}^\top QgK_I\tilde{x}_c \tag{3.2.7}$$

The next step is to calculate the time derivative of $\mathcal{V}_3$.

In this case, for the system equations, the controller state does not include a leakage term. The system state equations are given in (3.2.8).

$$\begin{cases} \dot{\tilde{x}} = (\mathcal{J}_o - \mathcal{R})Q\tilde{x} + g\tilde{u} \\ \dot{\tilde{x}}_c = -\hat{g}^\top Q\tilde{x} \end{cases} \tag{3.2.8}$$

And the controller is given in (3.1.8).

The time derivative is calculated:

$$\begin{aligned} \dot{\mathcal{V}}_3(\tilde{x}, \tilde{x}_c) &= \langle \nabla\mathcal{V}_3(\tilde{x}), f(\tilde{x}) \rangle + \langle \nabla\mathcal{V}_3(\tilde{x}_c), f(\tilde{x}_c) \rangle \\ &= \nabla\mathcal{V}_3^\top(\tilde{x}) \cdot \dot{\tilde{x}} + \nabla\mathcal{V}_3^\top(\tilde{x}_c) \cdot \dot{\tilde{x}}_c \end{aligned}$$

To find the expression of $\dot{\mathcal{V}}_3$, $\nabla\mathcal{V}_3$ is needed.

$$\nabla\mathcal{V}_3 = \begin{bmatrix} \frac{\partial V(\tilde{x}, \tilde{x}_c)}{\partial \tilde{x}} \\ \frac{\partial V(\tilde{x}, \tilde{x}_c)}{\partial \tilde{x}_c} \end{bmatrix} \tag{3.2.9}$$

The partial-derivative values are calculated respectively.

$$\nabla \mathcal{V}_3(\tilde{x}) = \frac{\partial}{\partial \tilde{x}} \mathcal{V}_3 = Q\tilde{x} - \varepsilon Q g K_I \tilde{x}_c$$
$$\nabla \mathcal{V}_3(\tilde{x}_c) = \frac{\partial}{\partial \tilde{x}_c} \mathcal{V}_3 = K_I \tilde{x}_c - \varepsilon \tilde{x}^\top Q g K_I$$

With the gradient of $\mathcal{V}_3$ identified, it is possible to obtain the expression for $\dot{\mathcal{V}}_3$:

$$\begin{aligned}
\dot{\mathcal{V}}_3(\tilde{x}, \tilde{x}_c) &= \nabla \mathcal{V}_3^\top(\tilde{x}) \cdot \dot{\tilde{x}} + \nabla \mathcal{V}_3^\top(\tilde{x}_c) \cdot \dot{\tilde{x}}_c \\
&= (\tilde{x}^\top Q - \varepsilon \tilde{x}_c^\top K_I g^\top Q)((\mathcal{J}_o - \mathcal{R})Q\tilde{x} + g\tilde{u}) + (\tilde{x}_c^\top K_I - \varepsilon K_I g^\top Q\tilde{x})(-\hat{g}^\top Q\tilde{x}) \\
&= -\tilde{x}^\top Q\mathcal{R}Q\tilde{x} - \tilde{x}^\top Q g K_P g^\top Q\tilde{x} + \tilde{x}^\top Q g K_I \tilde{x}_c - \varepsilon \tilde{x}_c^\top K_I g^\top Q\mathcal{F}_o Q\tilde{x} \\
&\quad + \varepsilon \tilde{x}_c^\top K_I g^\top Q g K_P g^\top Q\tilde{x} - \varepsilon \tilde{x}_c^\top K_I g^\top Q g K_I \tilde{x}_c - \tilde{x}_c^\top K_I \hat{g}^\top Q\tilde{x} + \varepsilon \tilde{x}^\top Q g K_I \hat{g}^\top Q\tilde{x}
\end{aligned}$$

Note that $\varepsilon K_I g^\top Q\tilde{x} = \varepsilon \tilde{x}^\top Q g K_I$, as it is a scalar.

And using $\bar{K}_I := g K_I \hat{g}^\top = \begin{bmatrix} 0 & K_I \\ 0 & 0 \end{bmatrix}$ and $\bar{Q} := g^\top Q g$ to condense the expression for $\dot{\mathcal{V}}_3$:

$$\dot{\mathcal{V}}_3 = -\tilde{x}^\top Q(\mathcal{R} + \bar{K}_P - \varepsilon \bar{K}_I)Q\tilde{x} + \tilde{x}^\top Q(g)K_I\tilde{x}_c - \tilde{x}_c^\top(\varepsilon g^\top Q(\mathcal{F}_o - \bar{K}_P) + \hat{g}^\top)Q\tilde{x} - \tilde{x}^\top Q(\varepsilon \bar{Q})K_I\tilde{x}_c \tag{3.2.10}$$

## 3.3 Concluding Remarks on *Preliminearies*

This chapter summarizes the work conducted in [1]. The system model is presented in this chapter. It is transformed to a pH representation and then shifted to an incremental form such that the system is considered for desired operating point. In addition to the system modeling, the proposed controller is presented and given in incremental form. The second part of this chapter considers the stability analyses of the proposed controller by Lyapunov's method. First, the system was proven GAS by the inclusion of a leakage term. An attempt was made to find an LFC such that the system, without the inclusion of leakage, was rendered GAS. The calculations for this LFC were not finished, as is continued in the work conducted in the master's thesis.

# Chapter 4

# Leakage in the Controller

This chapter continues with the result from section 3.2.2 in the preliminary project [1]; a stability certificate for the system model with a PI controller, using current error as input for the proportional channel and voltage error as input for the integral channel, was obtained with a condition of a constant leakage in the output. In this chapter, the system parameters are presented. Following this, the leakage term is calculated, and a simulation model is created in MATLAB Simulink to verify the mathematical proof. In addition, the deviation in the voltage output required by the constant leakage is observed.

## 4.1 The Leakage Term

The condition for GAS is given by the leakage term $D$:

$$D > \frac{1}{4}\left(\frac{1}{R+K_P}+\frac{1}{G}\right) \tag{4.1.1}$$

The value of $D$ depends on the constant values $R$ and $G$, which are the rated values for resistance and conductance in the circuit, and the proportional gain $K_P$, which is a scalar value that is decided through tuning for performance. $D$ is included as a negative term in the controller state $\dot{x}_c$.

## 4.2 System and Load Flow Analysis

The parameters for the circuit in figure 3.1 are given in table 4.1. These parameters are based on the power converters from [18], as they show a stable and realistic system. The values are used as parameters for the simulation model.

| | |
|---|---|
| $u$ | $20V$ |
| $L$ | $2.3mL$ |
| $C$ | $190\mu C$ |
| $R$ | $2.134\Omega$ |
| $G$ | $0.0227S$ |

Table 4.1: Converter parameters

The initial value of the input signal $u$ is included in table 4.1, as it was considered the open circuit voltage of the circuits [18]. For this circuit, $u$ is considered the input signal, and $i_o$ is used as open circuit current instead.

### 4.2.1 Load Flow Analysis

A load flow analysis is conducted to obtain reference values utilized in the simulations. The reference values were considered as the equilibrium points, denoted $\bar{(\cdot)}$, during the calculations in section 3.2.2. The equilibrium points are calculated by use of the state space model. Each vector field is set equal to zero to find the values when there is no energy flowing in the system, i.e., the equilibrium points.

$$0 = -\frac{R}{L}\bar{i}_L - \frac{1}{C}\bar{v}_C + \frac{1}{L}\bar{u} \tag{4.2.1}$$

$$0 = -\frac{1}{C}\bar{i}_L - \frac{G}{C}\bar{v}_C - \frac{1}{C}\bar{i}_o \tag{4.2.2}$$

However, a load flow analysis is not the objective of the master's thesis, and neither is designing a converter. Therefore, the reference values for both voltage and current are obtained by continuing to use the data from [18]. The values are given as $v_C^{\text{ref}} = 15V$ and ${i_L}^{\text{ref}} = 2.5A$. The value of the open-loop current is not given. Therefore, it has to be calculated from the reference values. Eqaution (4.2.2) is used, and the equilibirum values are set as $\bar{v}_c = v_c^{\text{ref}}$ and $\bar{i}_L = i_L^{\text{ref}}$. The equation for $i_o$ is given in (4.2.3):

$$i_o = i_L^{\text{ref}} - v_C^{\text{ref}} \cdot G \tag{4.2.3}$$

## 4.3 Simulation Results and Interpretation

The setup in Simulink consists of three parts: the load flow, the controller, and the system model.

### 4.3.1 Inital Values and Setup in Simulink

The capacitor voltage reference and open-loop current are initial values, $v_C^{\text{ref}} = 15V$ and $i_o = 2.16A$. These values are inputs to the load flow, where $u^{\text{ref}}$ and $i_L^{\text{ref}}$ are calculated.

The system's controller is given as $u$ in (3.1.6). For the simulations, the inputs for the controller channels are the error between the signals' response and their respective reference value.

$$u = -K_P(i_L - i_L^{\text{ref}}) + K_I x_c \tag{4.3.1}$$

$u^{\text{ref}}$ is used as a reference value for the controller signal, supposed there is no deviation for the output signal for $i_L$. In Simulink, $u^{\text{ref}}$ is calculated in the load flow, and the expression is obtained from (4.2.1). The signal for $u^{\text{ref}}$ has the reference values for current and voltage as variables: $u^{\text{ref}} = i_l^{\text{ref}} \cdot R + v_c^{\text{ref}}$.

The controller state $\dot{x}_c$ is defined as the negative deviation for $v_C$ and a leakage term for the state $x_c$:

$$\dot{x}_c = -(v_C - v_C^{\text{ref}}) - DK_I(x_c - x_c^{\text{ref}})$$

The system equations are given as in (3.1.1) with $u$ as input. And the system's outputs are the regulated responses for $v_C$ and $i_L$.

### 4.3.2 Simulation Results

The objective of the master's thesis is to demonstrate the stability of the closed-loop system. Consequently, the simulations are conducted for a specific set of controller gains obtained through

tuning initially. $K_P$ and $K_I$ are both set to 15. Once $K_P$ is determined, the value of $D$ is calculated using equation (4.1.1), and a minimum stability threshold of $D = 11.02$ is established.

The simulation time is T = 2 seconds. The reference for capacitor voltage, $v_C^{\text{ref}}$, changes three times to examine the impact on the system's stability. The initial value of $15V$, then after 0.5 seconds, the first step with an increase of $10V$, another second, a further increase of $15V$, and lastly, a voltage drop of $5V$ after 0.2 seconds.

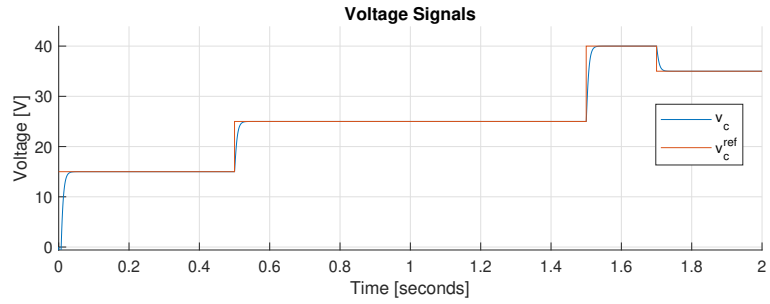


(a)

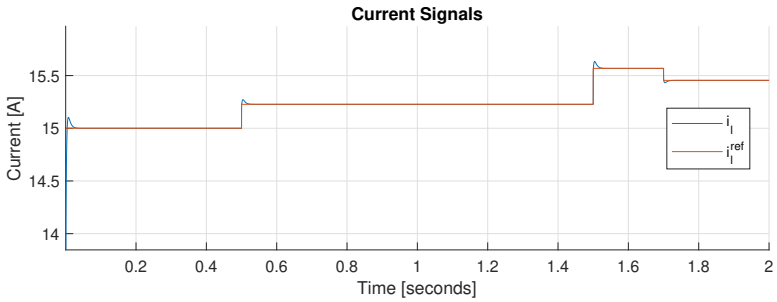


(b)

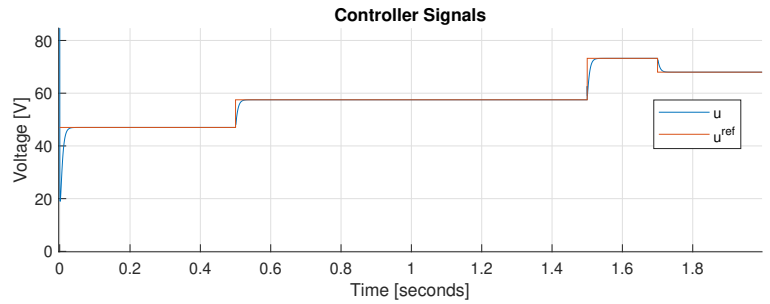


(c)

Figure 4.1: The system without deviation in $i_o$

In figure 4.1, the system's signal responses demonstrate no deviation from the reference values. The signal responses for $v_C$ and $u$ track their references without exhibiting oscillations and with a rapid settling time. Figure 4.1b illustrates the response of $i_L$, which exhibits a slight overshoot upon each step occurrence before quickly settling to its reference value. However, the magnitude of this overshoot is minimal, and the settling time is sufficiently short, resulting in a minimal impact on the system's stability.

These response behavior align with the expected initial behavior for a converter. However, as the device continues to regulate the responses, it is anticipated that the load flow will gradually lag behind the PI control, leading to deviations between the reference values from the load flow and from the controller into the system model. The system's leakage term would then appear as deviations in the voltage output.

**Deviaion Between the Reference Values into the Load Flow and into the System Model**

To show this in simulations, the open-circuit current $i_o$ is considered, as this is used as input to both the load flow and the system model. The value for $i_o$ into the system model is set to have a step after 0.9 seconds, while the value for $i_o$ used in the load flow calculations remains the same.

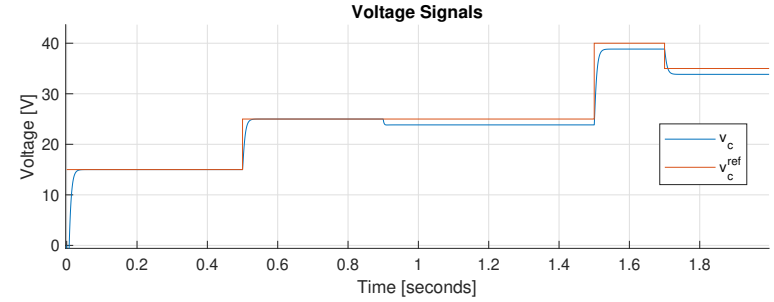


(a)

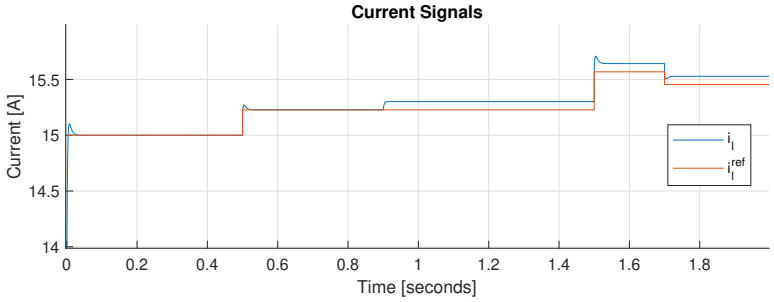


(b)

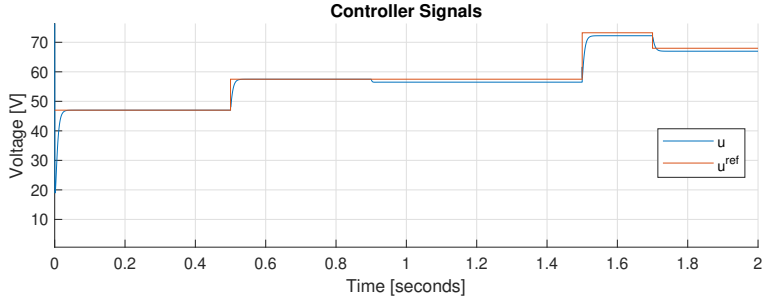


(c)

Figure 4.2: The system with some deviation in the open-circuit current $i_o$

In figure 4.2, a change in the reference value $i_o$ is introduced. For the initial 0.9 seconds in the simulation, the value for $i_o$ remains the same in the load flow and in the system. At t = 0.9 seconds, the input value for $i_o$ into the system is changed to $i_o = i_o + 0.1A$, while the value for $i_o$ into the load flow remains constant. As the signal responses for $v_C$ and $i_L$ from the system are fed back to the PI controller, a leakage will appear in the regulated responses.

The leakage term is introduced as a negative term in the voltage control. In figure 4.2a, the response for $v_C$ has a reduced value after t = 0.9 seconds. This is considered as a constant leakage for the output value, which remains for the rest of the simulation. The response for $v_C$ is not regulated such that it settles back into its reference value.

The response for $i_L$ shows a simultaneous increase in value in figure 4.2b. The difference between the responses for $v_C$ and $i_L$ and their respective reference value are approximately $1V$ and $74mA$.

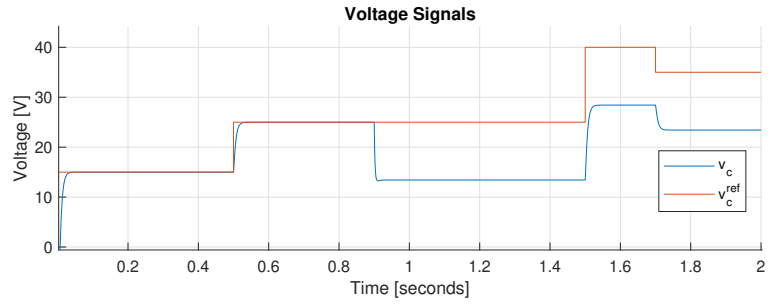


(a)

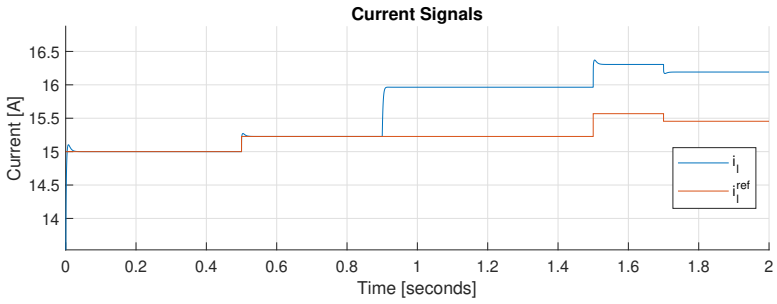


(b)

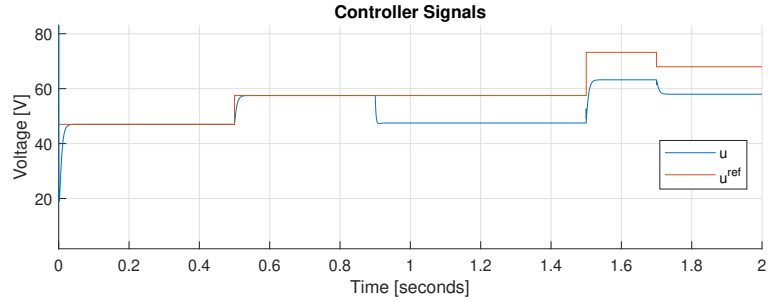


(c)

Figure 4.3: The system with deviation in the open-circuit current $i_o$

In figure 4.3, the deviation between the $i_o$-values is increased. At t = 0.9 seconds, the value for $i_o$ into the system is set to $i_o = i_o + 1A$ instead while the load flow's value remains. The leakage observed in the signal responses is significantly increased, as can be seen in figures 4.3a and 4.3b. The deviation in $i_o$ is only $1A$, but the effect on the output responses is consequential. The difference between the responses for $v_C$ and $i_L$ and their respective reference value are approximately $10V$ and $1A$.

## 4.4 Concluding Remarks on *Leakage in the Controller*

The closed-loop system in this chapter has a controller with a leakage term included. A simulation model was created using MATLAB Simulink, the model's parameters was obtained from [18], and the necessary reference and input values were calculated such that the simulation results show a stable system with and without voltage deviations. The deviations only appeared when there was a deviation between $i_o$ used as input to the load flow and to the system existed.

The output value for $v_C$ is the most affected by this leakage, especially when the deviation between $i_o$ for the system and the controller increases. This is due to the system being in voltage-control mode. In figure 4.3, it was observed that the required voltage deviations for the stabilizing term $D$ are not acceptable for practice, as the difference was $10V$.

# Chapter 5

# Populating the LFC

The process of populating the LFC began in [1] and is documented in section 3.2.2. Building upon the previous work conducted in [1], this chapter extends the calculations for the LFC. The objective remains unchanged: to determine suitable values for $\varepsilon$, as well as the tuning gains $K_P$ and $K_I$, such that $\dot{\mathcal{V}}_3 < 0$. The first part of this chapter focuses on completing the LFC calculations. Subsequently, efforts are made to ensure that the final inequality is greater than zero and that a Lyapunov function is obtained. Following these analyses, simulations are conducted for the system model.

## 5.1 Completing the Calculations for the LFC

In section 3.2.2 under *Populating the LFC*, the initial populating of a new LFC, denoted $\mathcal{V}_3$, was started. The proposed PI controller for this system model did not include the leakage term $D$. In [1], it was considered that the amount of leakage required would create voltage deviations that would not be considered acceptable in practice. Following, in chapter 4, simulations were conducted for this system and confirmed the assumption made in [1], as the voltage deviations were proven too great. Therefore, a new LFC is proposed to render the system without the inclusion of the leakage GAS. The calculations done in this chapter use the results from section 3.2.2 from [1] as a starting point.

A new LFC was designed, $\mathcal{V}_3$, and is given in (3.2.7). Its time-derivative $\dot{\mathcal{V}}_3$ (3.2.10) was calculated:

$$\mathcal{V}_3 = \frac{1}{2}\tilde{x}^\top Q\tilde{x} + \frac{1}{2}\tilde{x}_c^\top K_I\tilde{x}_c - \varepsilon\tilde{x}^\top QgK_I\tilde{x}_c$$
$$\dot{\mathcal{V}}_3 = -\tilde{x}^\top Q(\mathcal{R} + \bar{K}_P - \varepsilon\bar{K}_I)Q\tilde{x} + \tilde{x}^\top Q(g)K_I\tilde{x}_c - \tilde{x}_c^\top(\varepsilon g^\top Q(\mathcal{F}_o - \bar{K}_P) + \hat{g}^\top)Q\tilde{x} - \tilde{x}^\top Q(\varepsilon\bar{Q})K_I\tilde{x}_c$$

$\varepsilon$ is defined as a positive constant. Its exact value is unknown, but it is assumed to be small.

For $\mathcal{V}_3$ to be a Lyapunov function, then $\mathcal{V}_3 > 0$ and $\dot{\mathcal{V}}_3 < 0$. By calculating the Schur complement of both $\mathcal{V}_3$ and $\dot{\mathcal{V}}_3$, and show positive and negative definiteness, respectively, for a value of $\varepsilon$, a Lyapunov function is found. In section 3.2.2, $\mathcal{V}_3$ was populated such that it is a symmetric, positive definite matrix, given that $\varepsilon$ is a positive constant. Therefore, it is only necessary to calculate the Schur complement of $\dot{\mathcal{V}}_3$.

A condition for the Schur complement is that the matrix has to be symmetric. The symmetric part of $\dot{\mathcal{V}}_3$ is used for the calculations and obtained by use of (2.5.1).

The symmetric part of $\dot{\mathcal{V}}_3$ is calculated:

$$\frac{1}{2}\left(\begin{bmatrix} \mathcal{R}+\bar{K}_P-\varepsilon\bar{K}_I & -g \\ \varepsilon g^\top Q(\mathcal{F}_o-\bar{K}_P)+\hat{g}^\top & \varepsilon\bar{Q} \end{bmatrix} + \begin{bmatrix} (\mathcal{R}+\bar{K}_P-\varepsilon\bar{K}_I)^\top & \varepsilon(\mathcal{F}_o-\bar{K}_P)Qg+\hat{g} \\ -g^\top & \varepsilon\bar{Q} \end{bmatrix}\right)$$
$$= \begin{bmatrix} \mathcal{R}+\bar{K}_P-\frac{\varepsilon}{2}K_I^* & \frac{1}{2}(\varepsilon(\mathcal{F}_o-\bar{K}_p)Qg+\hat{g}-g) \\ \frac{1}{2}(\varepsilon(\mathcal{F}_o-\bar{K}_p)Qg+\hat{g}-g)^\top & \varepsilon\bar{Q} \end{bmatrix}$$

$\bar{K}_I \neq \bar{K}_I^\top$ and is not a symmetric matrix, like $\mathcal{R}$ and $\bar{K}_P$. Therefore, a new matrix $K_I^* = \begin{bmatrix} 0 & K_I \\ K_I & 0 \end{bmatrix}$ is introduced to condense the expression. The whole expression with the symmetric part of $\dot{\mathcal{V}}_3$ is given (5.1.1).

$$\dot{\mathcal{V}}_3 = -\begin{bmatrix} \tilde{x}^\top Q & \tilde{x}_c^\top K_I \end{bmatrix} \begin{bmatrix} \mathcal{R}+\bar{K}_P-\frac{\varepsilon}{2}K_I^* & \frac{1}{2}(\varepsilon(\mathcal{F}_o-\bar{K}_p)Qg+\hat{g}-g) \\ \frac{1}{2}(\varepsilon(\mathcal{F}_o-\bar{K}_p)Qg+\hat{g}-g)^\top & \varepsilon\bar{Q} \end{bmatrix} \begin{bmatrix} Q\tilde{x} \\ K_I\tilde{x}_c \end{bmatrix} \quad (5.1.1)$$

The Schur complement for $\dot{\mathcal{V}}_3$ in (5.1.1) will be calculated with respect to $\varepsilon\bar{Q}$, and therefore, $\mathcal{R}+\bar{K}_P-\frac{\varepsilon}{2}K_I^*$ has to be larger than zero and invertible. Due to the assumed low value of $\varepsilon$, the matrix is invertible (its determinant is larger than zero). All the conditions hold, and the Schur complement is calculated:

$$\varepsilon\bar{Q} - \frac{1}{4}(\hat{g}-g+\varepsilon(\mathcal{F}_o-\bar{K}_p)Qg)^\top(\mathcal{R}+\bar{K}_P-\frac{\varepsilon}{2}K_I^*)^{-1}(\hat{g}-g+\varepsilon(\mathcal{F}_o-\bar{K}_p)Qg) > 0 \quad (5.1.2)$$

If (5.1.2) holds for a valid $\varepsilon$, then $\dot{\mathcal{V}}_3$ is negative definite, and asymptotical stability is proved by $\mathcal{V}_3$. This is, however, not possible to determine immediately by observing the inequality as is. The unknown elements: $\varepsilon$, $K_P$, and $K_I$, give the problem. The issue presented with these values is to find an exact value for $\varepsilon$ that gives a positive Schur complement and find valid tuning gains for the controller.

It is proved difficult to find a valid $\varepsilon$ for the inequality in (5.1.2). Therefore, different adjustments are therefore considered to make the inequality true.

## 5.2 Investigating Solutions

To satisfy (5.1.2), $\varepsilon\bar{Q}$ must be greater than the product of the off-diagonal terms of the matrix and the inverse of the first element of the matrix. One possible approach is to set the gain of the proportional controller, $K_P$, to a very high value, as it appears in the inverse term. In this case, the product of the off-diagonal terms would be divided by a large value, resulting in a smaller magnitude compared to $\varepsilon\bar{Q}$. This possibility was considered and evaluated. However, due to the specific structure of $\bar{K}_P$, this approach does not yield the desired outcome. The high-valued $K_P$ is only present in the first element of the inverse matrix, as shown in (5.2.1).

$$\mathcal{R}+\bar{K}_P-\frac{\varepsilon}{2}K_I^* = \begin{bmatrix} R & 0 \\ 0 & G \end{bmatrix} + \begin{bmatrix} K_P & 0 \\ 0 & 0 \end{bmatrix} - \begin{bmatrix} 0 & \frac{\varepsilon}{2}K_I \\ \frac{\varepsilon}{2}K_I & 0 \end{bmatrix} = \begin{bmatrix} R+K_P & -\frac{\varepsilon}{2}K_I \\ -\frac{\varepsilon}{2}K_I & G \end{bmatrix} \quad (5.2.1)$$

The structure of (5.2.1) results in one of the terms in (5.1.2) not being divided by the high value of $K_P$. This is problematic because $\varepsilon\bar{Q}$, already a small value due to the small magnitude of $\varepsilon$, needs to be larger than the combined subtracting terms. Consequently, it becomes impossible to satisfy the inequality in (5.1.2).

### 5.2.1 Introducing $v$ in the Controller $\tilde{u}$

To adjust for this, a possibility is to remove the issue by mathematically adjusting the system to make the off-diagonal terms' contribution very small. And then implement this adjustment in the

system through the controller.

An attempt was made by multiplying the vectors $\hat{g} - g$ in (5.1.2) with a small factor $v$. This mathematical adjustment is given in (5.2.2).

$$\varepsilon\bar{Q} - \frac{1}{4}(v \cdot (\hat{g} - g) + \varepsilon(\mathcal{F}_o - \bar{K}_p)Qg)^\top (\mathcal{R} + \bar{K}_P - \frac{\varepsilon}{2}K_I^*)^{-1}(v \cdot (\hat{g} - g) + \varepsilon(\mathcal{F}_o - \bar{K}_p)Qg) > 0 \quad (5.2.2)$$

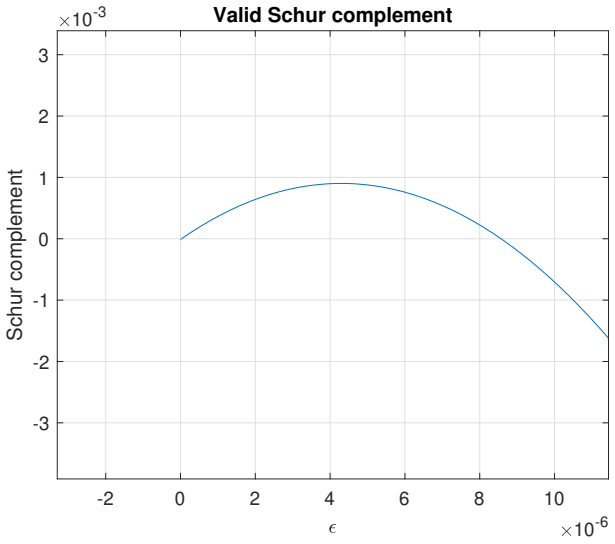


Figure 5.1: Area where both $\varepsilon$ and the inequality in (5.2.2) as a function of $\varepsilon$ are positive

For $v = 0.001$, $K_P = 10^3$ and $K_I = 10^{-3}$ in (5.2.2), it was possible to obtain a positive value for a region of $\varepsilon$-values, as shown in figure 5.1. However, this plot does not show proof of stability for the system because it is simply a mathematical adjustment. To make the inequality valid, $v$ has to be implemented in the system. As the goal is for $v$ to mainly affect the controller vectors, the controller and the controller state were adjusted. The controller $\tilde{u}$ is multiplied by $v$, giving a new controller $\tilde{w}$ (5.2.3).

$$\tilde{w} = v \cdot \tilde{u} = v \cdot (-K_P\tilde{y} + K_I\tilde{x}_c) \quad (5.2.3)$$

The change in the system equations is given in (5.2.4). The controller is changed to $\tilde{w}$, and $v$ is included in the controller state $\dot{\tilde{x}}_c$.

$$\begin{cases} \dot{\tilde{x}} = (\mathcal{J}_o - \mathcal{R})Q\tilde{x} + g\tilde{w} \\ \dot{\tilde{x}}_c = -v\hat{g}^\top Q\tilde{x} \end{cases} \quad (5.2.4)$$

It is necessary to calculate the time derivative of the LFC again to include all system changes. $\mathcal{V}_3$ is the same as in (3.2.7).

$$\begin{aligned}
\dot{\mathcal{V}}_3 &= (\tilde{x}^\top Q - \varepsilon\tilde{x}_c^\top K_I g^\top Q)((\mathcal{J}_o - \mathcal{R})Q\tilde{x} + g\tilde{w}) + (\tilde{x}_c^\top K_I - \varepsilon K_I g^\top Q\tilde{x})(-v\hat{g}^\top Q\tilde{x}) \\
&= -\tilde{x}^\top Q\mathcal{R}Q\tilde{x} - \tilde{x}^\top Qgv K_P g^\top Q\tilde{x} + \tilde{x}^\top Qgv K_I\tilde{x}_c - \varepsilon\tilde{x}_c^\top K_I g^\top Q(\mathcal{J}_o - \mathcal{R})Q\tilde{x} \\
&\quad + \varepsilon\tilde{x}_c^\top K_I g^\top Qgv K_P g^\top Q\tilde{x} - \varepsilon\tilde{x}_c^\top K_I g^\top Qgv K_I\tilde{x}_c - \tilde{x}_c^\top K_I v\hat{g}^\top Q\tilde{x} + \varepsilon\tilde{x}^\top Qg K_I v\hat{g}^\top Q\tilde{x} \\
&= -\tilde{x}^\top Q\left(\mathcal{R} + v\bar{K}_P - \varepsilon v\bar{K}_I\right)Q\tilde{x} + \tilde{x}^\top Q(vg)K_I\tilde{x}_c - \tilde{x}_c^\top K_I\left(\varepsilon g^\top Q(\mathcal{F}_o - v\bar{K}_P) + v\hat{g}^\top\right)Q\tilde{x} \\
&\quad - \tilde{x}_c^\top K_I(v \cdot \varepsilon\bar{Q})K_I\tilde{x}_c
\end{aligned}$$

The symmetric part main matrix $\dot{\mathcal{V}}_3$ is calculated for this case, as well:

$$\dot{\mathcal{V}}_3 = -\begin{bmatrix} \tilde{x}^\top Q \\ \tilde{x}_c^\top K_I \end{bmatrix}^\top \begin{bmatrix} \mathcal{R} + v\bar{K}_P - v \cdot \frac{\varepsilon}{2} K_I^* & \frac{1}{2}(\varepsilon(\mathcal{F}_o - v\bar{K}_P)Qg) + v(\hat{g} - g)) \\ \frac{1}{2}(\varepsilon(\mathcal{F}_o - v\bar{K}_P)Qg + v(\hat{g} - g))^\top & v \cdot \varepsilon\bar{Q} \end{bmatrix} \begin{bmatrix} Q\tilde{x} \\ K_I\tilde{x}_c \end{bmatrix} \tag{5.2.5}$$

As seen in (5.2.5), $v$ appears in front of the vectors $\hat{g} - g$, which was the goal. However, $v$ also appears with the gain matrices, $\bar{K}_P$ and $K_I^*$, and $\varepsilon\bar{Q}$. Using a small value for $v$ would mean the effect of the controller is barely there and will only lead to the need for very high tuning gains to have any effect from the controller. Also, the Schur complement is even more difficult to make valid as the term of the far left, $v \cdot \varepsilon\bar{Q}$, has to be the largest positive value for the inequality to hold, is even smaller than originally. The new Schur complement is given as in (5.2.6).

$$v\cdot\varepsilon\bar{Q} - \frac{1}{4}(v\cdot(\hat{g}-g)+\varepsilon(\mathcal{F}_o - v\bar{K}_p)Qg)^\top(\mathcal{R}+v\bar{K}_P - v\frac{\varepsilon}{2}K_I^*)^{-1}(v\cdot(\hat{g}-g)+\varepsilon(\mathcal{F}_o - v\bar{K}_p)Qg) > 0 \tag{5.2.6}$$

It was tried to obtain a positive result for (5.2.6), such as in figure 5.1. The new Schur complement was plotted with respect to $\varepsilon$, but it was only possible to obtain values for Schur that were close to zero or zero but never positive.

### 5.2.2 Increasing $G$

An alternative approach explored involves increasing the dissipation in the capacitor by raising the conductance value $G$ beyond its rated value. The remaining term in (5.1.2) will then be divided by a large value, and the resulting value will be small. If a small value is subtracted from $\varepsilon Q$, the inequality in (5.1.2) could be valid.

It should be noted that an increase in conductance, $G$, does not imply a modification in the device's actual rating. The additional conductance would be incorporated as a load in parallel to the capacitor. Although an augmented value of $G$ would result in increased losses within the component and diminish the overall impact of the converter, it is important to mention that this aspect falls outside the scope of this master's thesis. Consequently, the effects of this implementation are not explored further. The primary focus, however, centers around investigating whether this adjustment can provide evidence of asymptotic stability in the system.

The rated conductance value is $G = 0.0227S$. A higher $G$ is at some point expected to give a positive Schur complement even though the parameter is unrealistic high. Therefore, this value is increased substantially, and the respective Schur complements are calculated.

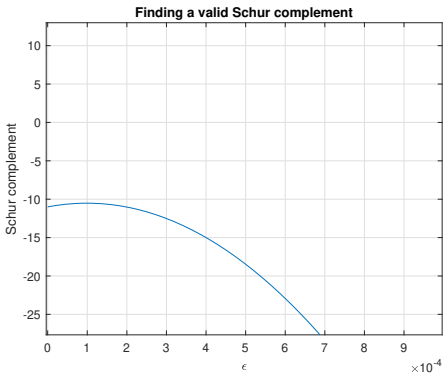


(a) $G = \frac{1}{44}S = 0.0227S$

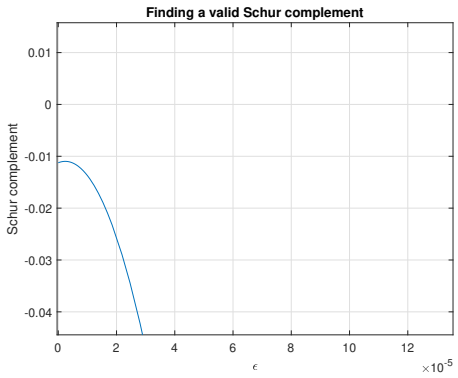


(b) $G = \frac{1}{44} \cdot 10^3 S = 22.72S$

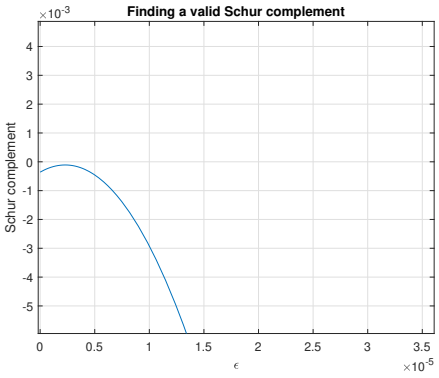


(c) $G = \frac{1}{44} \cdot 10^5 S = 2.27kS$

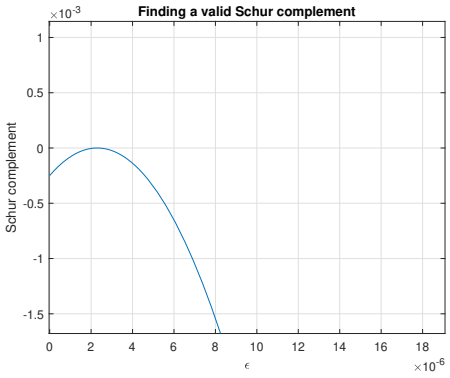


(d) $G = \frac{1}{44} \cdot 10^{10} S = 2.27 \cdot 10^7 S$

Figure 5.2: The value of the conductance $G$ is increased in an attempt to obtain a positive Schur complement

$G$ is set to four different values: $0.0227S$, $22.72S$, $2.27kS$, and $2.27 \cdot 10^7 S$, while the other parameters, $K_P$, and $K_I$, remain the same: $K_P = 10^3$ and $K_I = 10^{-3}$. The respective Schur complements are calculated and plotted for each value $G$ and shown in subfigures (a)-(d) in figure 5.2.

Figure 5.2a shows the inequality for the rated value of $G$. It is far from positive, even though the value of $\varepsilon$ is small. Therefore, changing $G$ to a higher value could potentially give a positive value to the function. Continuing in figure 5.2b, an increase in $G$ gives an observable effect on the function. It has become less negative and is closing in on the line, indicating zero. The next figure, 5.2c, shows a function that almost touches the zero line. And lastly, with an unrealistic high value of $G$, the function touches the zero line but does not become a positive value. It was also checked for an even higher $G$, but the function did not obtain any higher value than zero.

## 5.3 A New Lyapunov Function Candidate

In section 5.2, several attempts were made to design an LFC by populating the unknown terms of $\mathcal{V}_3$, with the goal of obtaining $\dot{\mathcal{V}}_3$ negative definite. Neither a small adjustment in the controller nor increasing $G$ worked, and, therefore, the system was considered from an alternative standpoint. Since the system has linear dynamics, it is possible to consider the system's state matrix and the Lyapunov equation to find a Lyapunov function that gives a stable system.

### 5.3.1 Using the Lyapunov Equation to Show Stability

To use the Lyapunov equations given in (2.7.1) and find a Lyapunov function, the state matrix $A_{pop}$ for (3.2.8) has to be calculated. Using the controller (3.1.8), the system's closed-loop states

are then given as:

$$\begin{aligned}\dot{\tilde{x}} &= \begin{bmatrix}\dot{\tilde{\Phi}}_L \\ \dot{\tilde{q}}_C\end{bmatrix} = \begin{bmatrix}-\frac{R}{L} & -\frac{1}{C} \\ \frac{1}{L} & -\frac{G}{C}\end{bmatrix}\begin{bmatrix}\tilde{i}_L \\ \tilde{v}_C\end{bmatrix} + \begin{bmatrix}-K_P\frac{\tilde{i}_L}{L} + K_I\tilde{x}_c \\ 0\end{bmatrix} \\ &= \begin{bmatrix}-R\tilde{\Phi}_L - \frac{1}{C}\tilde{q}_C - \frac{K_P}{L}\tilde{\Phi}_L + K_I\tilde{x}_c \\ \frac{1}{L}\tilde{\Phi}_L - \frac{G}{C}\tilde{q}_C\end{bmatrix} \\ \dot{\tilde{x}}_c &= -\frac{1}{C}\tilde{q}_C\end{aligned}$$

By use of the system's differential equations and of the system's states, $\tilde{\Phi}_L$, $\tilde{q}_C$, and $\tilde{x}_c$, $A_{pop}$ is given in (5.3.1).

$$A_{pop} = \begin{bmatrix}-\frac{R+K_P}{L} & -\frac{1}{C} & K_I \\ \frac{1}{L} & -\frac{G}{C} & 0 \\ 0 & -\frac{1}{C} & 0\end{bmatrix} \tag{5.3.1}$$

Using a high value of the proportional gain, $K_P = 10^3$. The eigenvalues of $A_{pop}$ are calculated and given in table 5.1.

| $\lambda_i$ | Eigenvalue |
|---|---|
| $\lambda_1$ | $-4.3571 \cdot 10^5$ |
| $\lambda_2$ | $-124.871$ |
| $\lambda_3$ | $-0.4206 \cdot 10^{-5}$ |

Table 5.1: Eigenvalues of $A_{pop}$

$A_{pop}$ is Hurwitz since all the eigenvalues in table 5.1 are negative, and $\mathcal{Q}$ is set equal to the identity matrix, $\mathcal{Q} = \mathcal{I}_3$, which makes it positive definite. The conditions for using (2.7.1) hold, and the matrix $\mathcal{P}$ is calculated:

$$\mathcal{P} = \begin{bmatrix}1.7318 \cdot 10^{-6} & -4.8354 \cdot 10^{-4} & 0.0485 \\ -4.8354 \cdot 10^{-4} & 0.004 & 9.5 \cdot 10^{-5} \\ 0.0485 & 9.5 \cdot 10^{-5} & 2.1132 \cdot 10^7\end{bmatrix} \tag{5.3.2}$$

Since $\mathcal{P}$ also is positive definite, it is a valid Lyapunov function for (3.2.8) and proves that the system is asymptotically stable.

Using $\tilde{x}^\top = \begin{bmatrix}\tilde{\Phi}_L & \tilde{q}_c\end{bmatrix}$, the numerical Lyapunov function is given as in (5.3.3).

$$\mathcal{V}_4(\tilde{x}) = \begin{bmatrix}\tilde{x}^\top & \tilde{x}_c^\top\end{bmatrix}\begin{bmatrix}1.7318 \cdot 10^{-6} & -4.8354 \cdot 10^{-4} & 0.0485 \\ -4.8354 \cdot 10^{-4} & 0.004 & 9.5 \cdot 10^{-5} \\ 0.0485 & 9.5 \cdot 10^{-5} & 2.1132 \cdot 10^7\end{bmatrix}\begin{bmatrix}\tilde{x} \\ \tilde{x}_c\end{bmatrix} \tag{5.3.3}$$

And the time-derivative of $\mathcal{V}_4$:

$$\dot{\mathcal{V}}_4(\tilde{x}) = -\begin{bmatrix}\tilde{x}^\top & \tilde{x}_c^\top\end{bmatrix}\begin{bmatrix}1 & 0 & 0 \\ 0 & 1 & 0 \\ 0 & 0 & 1\end{bmatrix}\begin{bmatrix}\tilde{x} \\ \tilde{x}_c\end{bmatrix} \tag{5.3.4}$$

### 5.3.2 Compared to the Previous LFC

The LFC $\mathcal{V}_3$ (3.2.7) proposed in sections 3.2.2 and 5.2 did not show asymptotic stability. By observation of (5.3.2), it is possible to obtain some insight into how $\mathcal{V}_3$ could be revised to give asymptotic stability. $\mathcal{V}_3$ is given in matrix form in (5.3.5).

$$\mathcal{V}_3 = \begin{bmatrix} \tilde{\Phi}_L^\top & \tilde{q}_C^\top & \tilde{x}_c^\top \end{bmatrix} \underbrace{\begin{bmatrix} \frac{1}{L} & 0 & -\frac{\varepsilon}{L}K_I \\ 0 & \frac{1}{C} & 0 \\ -\frac{\varepsilon}{L}K_I & 0 & K_I \end{bmatrix}}_{\mathcal{M}} \begin{bmatrix} \tilde{\Phi}_L \\ \tilde{q}_C \\ \tilde{x}_c \end{bmatrix} \tag{5.3.5}$$

The elements of $\mathcal{M}$ which haven't already been altered are $\mathcal{M}_{(1,2)}$ and $\mathcal{M}_{(2,1)}$. In the case of stability, $\mathcal{P}$, these values are non-zero and small. An adjustment of $\mathcal{V}_3$ is done by setting the zero values to $a$, a small positive constant.

$$\mathcal{M}^* = \begin{bmatrix} \frac{1}{L} & a & -\frac{\varepsilon}{L}K_I \\ a & \frac{1}{C} & 0 \\ -\frac{\varepsilon}{L}K_I & 0 & K_I \end{bmatrix}$$

However, due to time limitations, further efforts to determine a value for $a$ have not been pursued.

## 5.4 Simulation Results and Interpretation

The closed-loop system without the inclusion of leakage term was rendered GAS by a Lyapunov function obtained by use of the Lyapunov equation. Because proof of stability is obtained, simulations of the system are conducted to show the dynamics of the system.

### 5.4.1 Initial Values and Setup in Simulink

The setup for the simulation is the same as in section 4.3, with three parts: open-loop load flow, controller, and system equations. The open loop load flow and the controller remain the same. $v_C^{ref}$ and $i_o$ are inputs, and $i_L^{ref}$ and $u^{ref}$ are the outputs in the load flow, and the controller is given in (4.3.1). The system in this chapter is not considered for leakage, the leakage term is therefore neglected, and the virtual controller state $\dot{x}_c$ is only given as the negative error signal for $v_C$.

$$\dot{x}_c = -(v_C - v_C^{ref}) \tag{5.4.1}$$

The system equations are given in (3.1.1) with $u$ as input, and the system's outputs are the responses for $v_C$ and $i_L$.

### 5.4.2 Simulation Results

The gains are tuned briefly for the new system and then set to constant values, $K_P = 50$ and $K_I = 15$. The system with these gains follows the reference but has a longer settling time, so in case of quick changes, the response does not manage to settle into its reference value. Also, it was important that the controller signal remained within reasonable values whenever a step in the reference value was introduced. However, the system is considered stable as there are no oscillations or overshoots, and the responses follow their references.

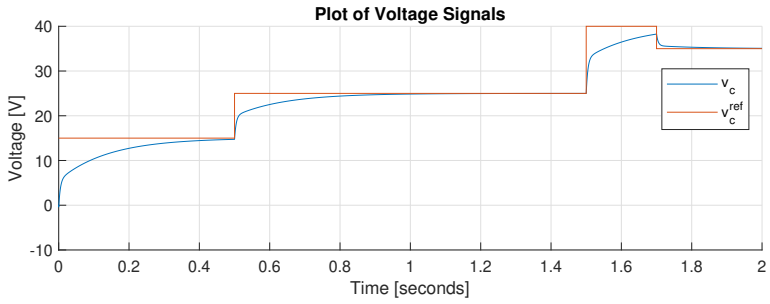


(a)

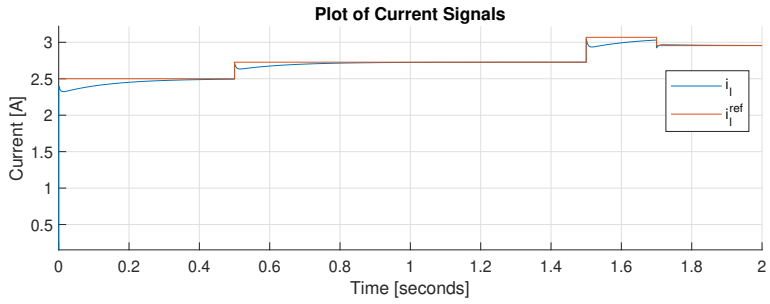


(b)

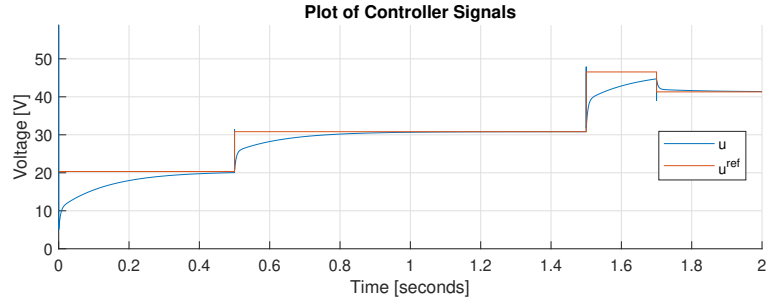


(c)

Figure 5.3: The system without any altering

Figure 5.3 shows plots of the $v_C$, $i_L$, and $u$ responses compared to the respective reference signal. As expected, due to the limited tuning, the responses are slow but follow the reference signals. The system has no oscillations before the response settles into the reference. The only noteworthy disturbance is given in figure 5.3c; when a step occurs, the controller signal $u$ has a small value spike before it drops and then starts to settle into the reference value. In the case of stability, the spikes are very low, but if they become extremely high, this means instability. The controller's signal is a voltage signal, and a converter is not dimensioned for this value to rise to extremely high values. For the response of $u$, there is also a high rise in value immediately when the device is turned on, this is ignored since this is only a simulation, and for the real case, filters or other measures are in place for the start-up to avoid this high rise in value.

### 5.4.3 Increasing $G$

Considering (5.1.2), it was assumed that an increased value $G$ would make the inequality hold at some point. However, the function of the inequality in (5.1.2) seemed only to approach zero and not become a positive value, no matter how great the value of $G$.

In the case for simulations, three different values for $G$ are considered: the rated value $\frac{1}{44} = 0.2273S$,

$G = 22.73S$, and $G = 2.273kS$. From the simulations, only plots of the $v_C$ responses with their reference signals are included. The PI controller is in voltage-control mode. Therefore, it is relevant to see how increased values for $G$ affect the control of $v_C$. Additionally, the values for $i_L$ and $u$ will only show extremely high values and instability as the conductance value is raised to unrealistically high values.

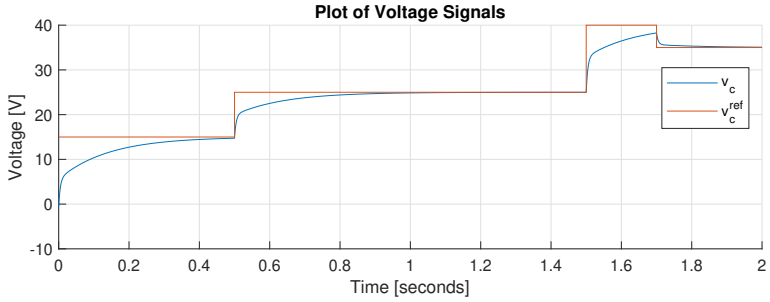


(a) $G = \frac{1}{44}$

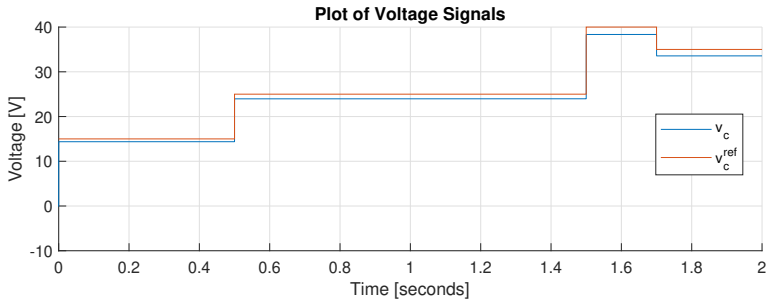


(b) $G = \frac{1}{44} \cdot 10^3$

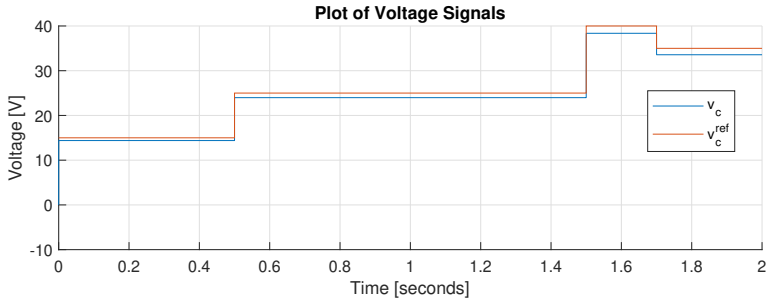


(c) $G = \frac{1}{44} \cdot 10^5$

Figure 5.4: Comparing responses of $v_C$ with different values of the conductance $G$

When the value of $G$ is increased, the responses for $v_C$ are improved without the need for tuning, as observed in 5.4. Even though the regulation of $v_C$ is improved by higher $G$, the system is not improved as a whole because of the problems for $i_L$ and especially $u$. These simulations are included as a supplement to the calculations section 5.2.2.

### 5.4.4 System Dynamics Considered for Deviation in the Open-Circuit Current $i_o$

In this section, the conductance $G$ is set to its rated value. In section 4.3, the system's response was checked when the input values in the system deviated from the input in the load flow. In the case of this system, the controller is expected to regulate the responses back to the reference values and not have a constant deviation in the output.

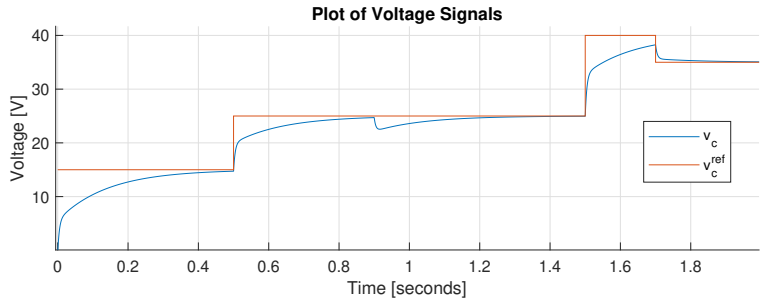


(a)

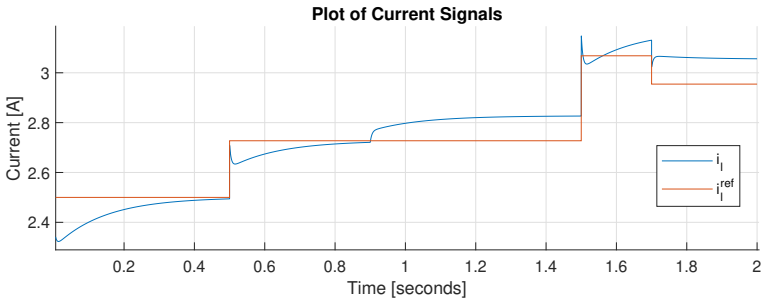


(b)

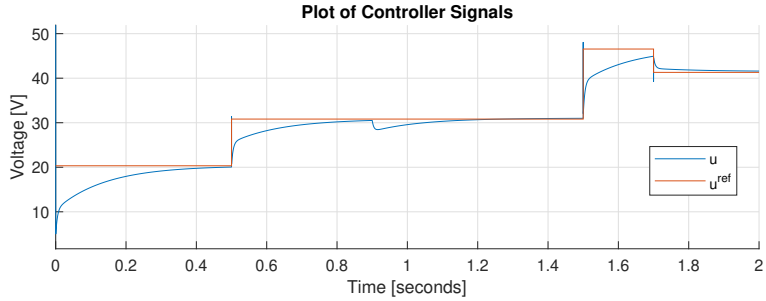


(c)

Figure 5.5: The system with some deviation in the open-circuit current $i_o$

Figure 6.4 shows the system's responses when $i_o$ into the system is different from the value into the load flow. At t = 0.9 seconds, the input value in the system is increased to $i_o = i_o + 0.1A$. The response for $v_C$ and $u$ drops at t = 0.9 seconds but quickly settle into their reference value again. However, the response for $i_L$ does not settle into its reference after t = 0.9 seconds, as seen in figure 5.5b. It deviates with approximately $0.1A$. The lack of regulation in the response for $i_L$ is due to the PI controller operating in voltage-control mode, and there is no integral effect to regulate the response for $i_L$.

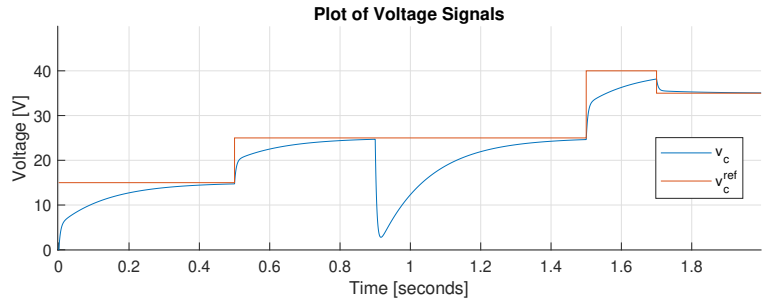


(a)

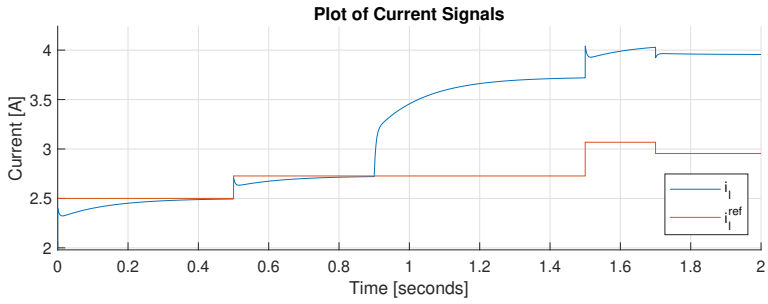


(b)

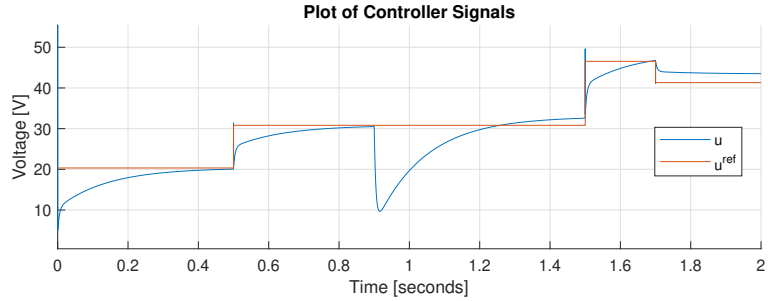


(c)

Figure 5.6: The system with deviation in the open-circuit current $i_o$

In figure 5.6, the input of $i_o$ into the system is increased to $i_o = i_o + 1A$. This change makes for a drop in value for the responses of $v_C$ and $u$. This change is quickly regulated, and the response settles into its reference value after 0.2 seconds for $u$ and after 0.4 seconds for $v_C$. The response of $i_L$ does not manage to settle into its reference. The response is approximately $2A$ higher than the reference. Again, due to no integral effect for the error in the response of $i_L$.

## 5.5 Concluding Remarks on *Populating the LFC*

The proposed way of populating an LFC and then determining the unknown values such that the conditions for the Lyapunov method are upheld was not possible. However, the system is GAS, and a numerical Lyapunov function was found. The numerical Lyapunov function helped identify issues in the populated LFC, which contributed to modifications of the proposed LFC.

As the system was proven GAS by the numerical Lyapunov function, simulations were conducted to observe the system dynamics. By increasing $G$, the inequality in (5.1.2) obtained a higher value, but never a high enough value to become positive. Simulations with different high values of $G$ affected the response for $v_C$ positively, but if the responses for $u$ and $i_L$ were considered, the system was unstable.

For the system dynamics, when the open-circuit $i_o$ deviated in the load flow and the system equations, the voltage responses, $v_C$, and $u$, were regulated to the reference values. In contrast, the response for $i_L$ did not correct itself, which is due to the PI controller operating in voltage-control mode and no integral effect removing the error in the current response.

# Chapter 6

# Leakage in the Controller and the Populated LFC Combined

This chapter investigates the proposed PI controller from section 3.2.2 and chapter 4, which includes a leakage term within the controller, as well as the populated LFC discussed in section 3.2.2 and chapter 5. More precisely, the system equations in (3.2.4), the controller in (3.1.8), and the LFC $\mathcal{V}_3$ in (3.2.7) to prove GAS. The chapter begins with the motivation behind the proposed system, followed by the calculation of the time derivative of the Lyapunov function to demonstrate GAS. Additionally, a new stabilizing condition is determined for the leakage term to minimize voltage deviations in the system's output.

## 6.1 Motivation for the Proposed System

In section 3.2.2 and chapter 4, a GAS system required the inclusion of a leakage term in the controller, which necessitated voltage deviations for the system's output. Additionally, the proposed LFC presented in chapters 3 and 5 did not demonstrate asymptotical stability for the system without including leakage, as the necessary constants for the function appeared not to exist. As a compromise between the applied methods, the LFC (3.2.7) is utilized in this chapter to establish asymptotical stability for the system, including a leakage term, while obtaining acceptable levels of voltage deviations by increasing the value of the conductance $G$.

In section 5.2.2, the conductance $G$ was raised to values beyond its rated capacity in an attempt to establish asymptotic stability. Regrettably, even with unrealistically high values, the system remained unstable. However, based on the functions plotted in figure 5.2, an increased value of $G$ exhibited an observable effect to render the Schur complement of $\dot{\mathcal{V}}_3$ positive (or negative definite if a negative sign is applied).

The approach pursued in this chapter involves utilizing the leakage term $D$ derived from chapter 4 to compute a positive Schur complement for the time derivative of the LFC. This computation aids in determining a suitable value for $\varepsilon$ for an increased conductance value $G$. Furthermore, by incorporating the values of $\varepsilon$ and $G$, a new stabilizing condition for the leakage term is established. Subsequently, the modified leakage term $D$ and the increased value of $G$ are utilized in the simulation model to reduce the required voltage deviations for the system to be asymptotically stable.

## 6.2 Calculations for the Proposed System and Increasing the Conductance $G$

The initial calculations in this chapter are expected to prove asymptotically stable because the system, including a leakage, was proven GAS in [1], as seen in section 3.2.2 and the LFC $\mathcal{V}_3$ was inspired by the results from this stability analysis.

The system equations are given in (3.2.4) and the controller in (3.1.8). The proposed Lyapunov function is $\mathcal{V}_3$, (3.2.7). The time-derivative of $\mathcal{V}_3$ is calculated:

$$\begin{aligned}\dot{\mathcal{V}}_3 &= (\tilde{x}^\top Q - \varepsilon\tilde{x}_c^\top K_I g^\top Q)((\mathcal{J}_o - \mathcal{R})Q\tilde{x} + g\tilde{u}) + (\tilde{x}_c^\top K_I - \varepsilon\tilde{x}^\top Q g^\top Q\tilde{x})(-\hat{g}^\top Q\tilde{x} - DK_I\tilde{x}_c)\\ &= -\tilde{x}^\top Q(\mathcal{R} + \bar{K}_P - \varepsilon\bar{K}_I)Q\tilde{x} - \tilde{x}^\top Q(-g - \varepsilon\hat{g}K_I D)K_I\tilde{x}_c - \tilde{x}_c^\top K_I(\varepsilon g^\top Q(\mathcal{F}_o - \bar{K}_P) + \hat{g}^\top)Q\tilde{x}\\ &\quad - \tilde{x}_c^\top K_I(\varepsilon\bar{Q} + D)K_I\tilde{x}_c\end{aligned}$$

Written as the symmetric part of the matrix:

$$\dot{\mathcal{V}}_3 = \begin{bmatrix}\tilde{x}^\top Q\\ \tilde{x}_c^\top K_I\end{bmatrix}^\top \begin{bmatrix}\mathcal{R} + \bar{K}_P - \varepsilon\bar{K}_I & \frac{1}{2}\left(\varepsilon(\mathcal{F}_o - \bar{K}_P)^\top Qg + \hat{g} - g - \varepsilon K_I D\hat{g}\right)\\ \frac{1}{2}\left(\varepsilon g^\top Q(\mathcal{F}_o - \bar{K}_P) + \hat{g}^\top - g^\top - \varepsilon K_I D\hat{g}^\top\right) & \varepsilon\bar{Q} + D\end{bmatrix}\begin{bmatrix}\tilde{x}^\top Q\\ \tilde{x}_c^\top K_I\end{bmatrix} \tag{6.2.1}$$

$\dot{\mathcal{V}}_3$ expressed as a symmetric matrix, and $\mathcal{R} + \bar{K}_P - \varepsilon\bar{K}_I$ is invertible, the Schur complement for $\dot{\mathcal{V}}_3$ is calculated directly as in (2.6.2):

$$\varepsilon\bar{Q} + D - \frac{1}{4}(\varepsilon g^\top Q(\mathcal{F}_o - \bar{K}_P) + (\hat{g} - g)^\top - \varepsilon K_I D\hat{g}^\top)(\mathcal{R} + \bar{K}_P - \varepsilon\bar{K}_I)^{-1}(\varepsilon(\mathcal{F}_o - \bar{K}_P)^\top Qg + \hat{g} - g - \varepsilon K_I D\hat{g}) > 0 \tag{6.2.2}$$

To calculate the Schur complement in (6.2.2) and find a value for $\varepsilon$, the system parameters are given in table 4.1. In addition to this table, table 6.1 is created. This table includes the proportional controller gain $K_P$ and the leakage term $D$, as well as the undecided value $\varepsilon$ and the conductance $G$. The values in table 6.1 will be updated in this chapter as the adjustment and calculations are made.

| | |
|---|---|
| $G$ | $0.0227S$ |
| $K_P$ | 15 |
| $D$ | 11.02 |
| $\varepsilon$ | - |

Table 6.1: Initial parameters

The Schur complement is calculated twice; first for the normal value of $G$, as given in tables 4.1 and 6.1, and second for an increased value of $G = 22.72S$ while the other parameters remain constant.

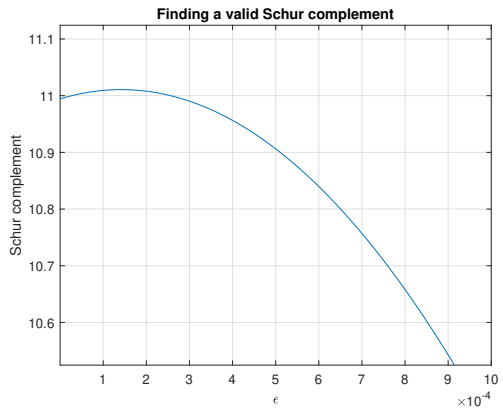


(a) Normal value of $G$


(b) Increased value of $G$

Figure 6.1: The Schur complement as a function of $\varepsilon$ is calculated twice: for $G = 0.0227S$ in (a) and for $G = 22.73S$ in (b)

Both plots in figure 6.1 show a positive value of the Schur complement, and this means GAS systems for both values of $G$. The values of $\varepsilon$ give positive function values in a wide range, and a common value for both plots is chosen: $\varepsilon = 2 \cdot 10^{-4}$. In other words, this value of $\varepsilon$ can be used in the same LFC and render both systems stable.

With a decided value of $\varepsilon$, the Schur complement is considered as a function of the leakage term $D$ instead. And in hopes of finding a new, lower stabilizing condition for the leakage term, the new Schur complement is calculated. The parameters used in this calculation are given in table 6.2.

| | |
|---|---|
| $G$ | $22.73S$ |
| $K_P$ | 15 |
| $D$ | - |
| $\varepsilon$ | $2 \cdot 10^{-4}$ |

Table 6.2: Updated parameters

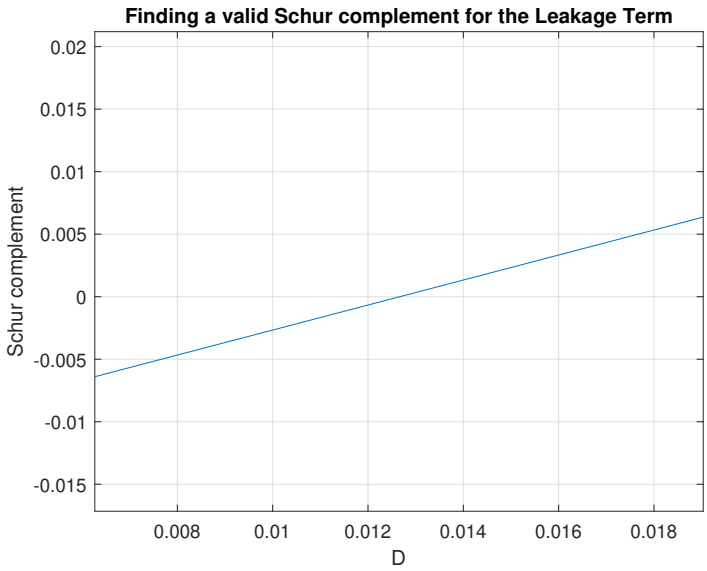


Figure 6.2: The Schur complement as a function of $D$

Based on the resulting function in figure 6.2, the Schur complement is definitely positive when

the leakage term is more than $D > 0.013$. By setting $D = 0.014$, the system is guaranteed GAS. Compared to the previous leakage term of 11.02 from chapter 4, the voltage deviations required for stability for this system are considerably lower. If the actual deviations are considered suitable for practice will be given by simulation results.

With the new value for conductance, the leakage term of $D$ can be calculated using the stabilizing condition found in section 3.2.2, for the previous LFC used for the leakage system, $\mathcal{V}_2$. Equation (4.1.1) is used and gives the stabilizing condition for $D > 0.026$. Because the condition for GAS obtained by use of $\mathcal{V}_3$ is lower, this will probably reduce the voltage deviations the most and is considered for further analysis.

| | |
|---|---|
| $G$ | $22.73S$ |
| $K_P$ | 15 |
| $D$ | 0.014 |
| $\varepsilon$ | $2 \cdot 10^{-4}$ |

Table 6.3: The final update of parameters to be used in the simulation model and the Lyapunov function

## 6.3 Simulation Results and Interpretation

The findings presented in section 6.2 demonstrate a GAS system that incorporates a leakage term, requiring reduced voltage deviations, compared to chapter 4, for the stability condition to be met. However, this achievement comes at the expense of a high dissipation, precisely the conductance value $G$. In this system, the rated value of $G$ provided in table 4.1 is multiplied by a factor of $10^3$. It is important to note that increasing this value results in amplified output losses. Nonetheless, since the scope of this master's thesis does not encompass considerations beyond theoretical analysis, the practical feasibility of such an approach is not explored.

### 6.3.1 Initial Values and Setup in Simulink

The simulations model developed in section 4.3 is considered for the simulations conducted in this section as well, as the system equations and controller are the exact same. However, the value for $G$ and $D$ is updated according to the values in table 6.3. The controller gains $K_P$ and $K_I$ remain the same as in section 4.3, i.e., $K_P = K_I = 15$.

### 6.3.2 Simulations results

#### System without change in $i_o$

A normal simulation of the system model is conducted. The reference values into the load flow and into the system model match, and the leakage is not expected to be observed in terms of voltage deviation for this case.

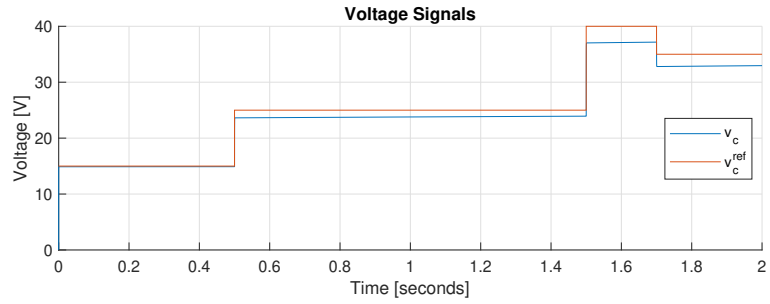


(a)

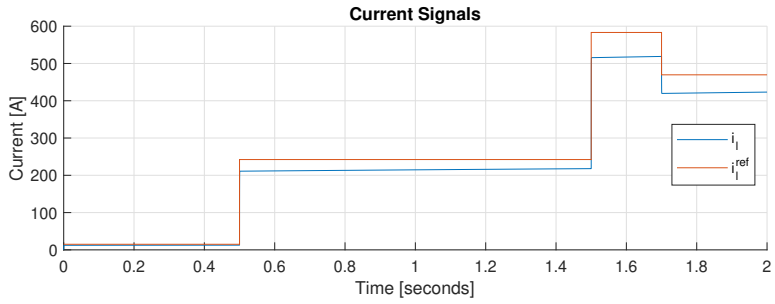


(b)

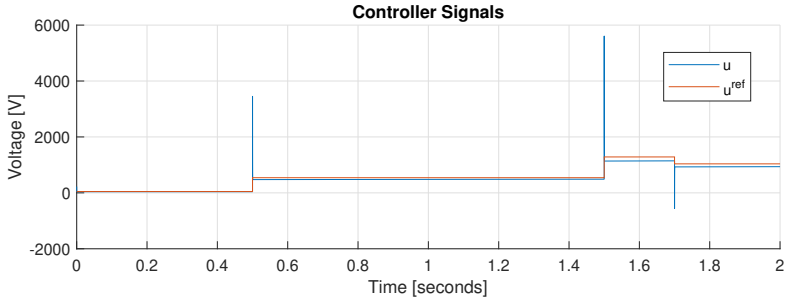


(c)

Figure 6.3: The system without any altering

With an increased conductance value, it is clear that the system is no longer tuned for performance for $K_P = K_I = 15$. However, the signal responses follow their respective references with some deviation that remains constant for all three responses: $v_C$, $i_L$, and $u$. A higher value of the tuning gain $K_P$ will remove this issue.

As mentioned previously, a higher dissipation is expected to amplify the system's losses, and with the high values of $i_L$, as seen in figure 6.3b, this assumption is confirmed. However, another issue with the increased value of $G$ occurs for the controller signal $u$; for each step in $v_C^{\text{ref}}$, high spikes occur. This issue was also mentioned in section 5.4.3 but neglected as the simulations were considered for $v_C$. As this is a voltage signal, it is an issue to dimension a converter to sustain such high values. The use of a high conductance value gives stability issues, which is expected.

### System with change in $i_o$

For the leakage to be expressed, a mismatch of the reference values for load flow and the system model is introduced. The input for $i_o$ to the load flow remains, while the value for $i_o$ into the system equations is $i_o = i_o + 1A$. The mismatch is initiated at t = 0.9 seconds.

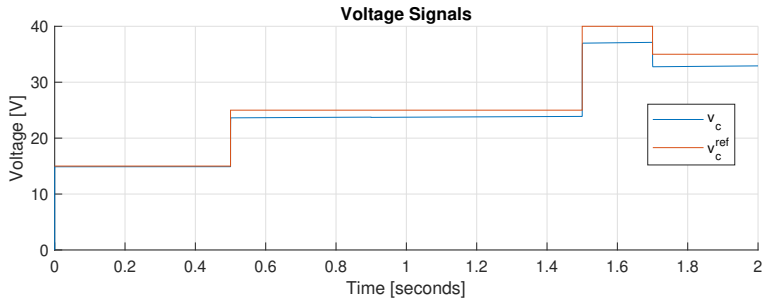


(a)

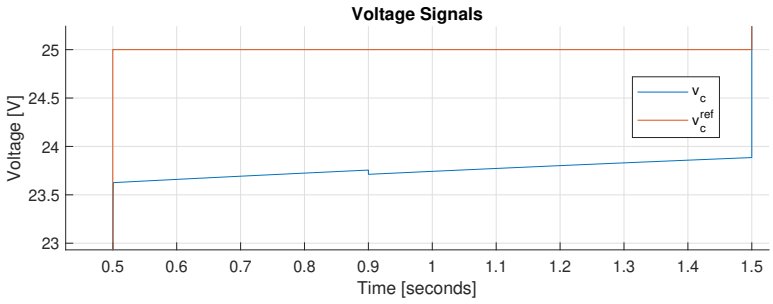


(b)

Figure 6.4: The system with deviation in the open-circuit current $i_o$

The voltage deviation due to the leakage term affects the whole system, but as the system works in voltage-control mode, the response for $v_C$ is of interest. Figure 6.4a shows the plot of $v_C$, the change for $i_o$ is initiated at t = 0.9 seconds. However, in this plot, no apparent changes are observable. By comparing figure 6.3a and figure 6.4a, the responses for $v_C$ are the same. A zoomed-in plot of the response for $v_C$ is given in figure 6.4b. At exactly t = 0.9 seconds, a small change appears in the response for $v_C$, but this change is minimal and does not affect the output value. It, however, seems like the regulator tries to improve the signal for $v_C$ until the next step in reference happens.

By using the increased value of $G$ and the new stabilizing condition for the leakage term, it was possible to minimize the voltage deviations in the output, however, at the expense of increased losses in the system and higher spikes in the control signal response. However, the chosen approach successfully reduces the necessary voltage deviations within this particular context and is therefore included, even though the response for $u$ is not acceptable.

## 6.4 Concluding Remarks on *Leakage in the Controller and the Populated LFC Combined*

The proposed system and Lyapunov function in this chapter was considered to reduce the voltage deviations required by the leakage term by an increased value of $G$. $G$ was increased to $22.73S$, instead of $0.0227S$, and the Lyapunov function rendered the system GAS. A valid value for $\varepsilon = 2 \cdot 10^4$ in $\mathcal{V}_3$ was considered, and then a new stabilizing condition for the leakage term was obtained. It was set to $D = 0.014$, instead of 11.02, and simulations were conudcted to observe if the voltage deviations were reduced. Subsequently, the simulations showed minimal deviations in the response for $v_C$.

# Chapter 7

# Conclusion and Future Works

This chapter presents the general conclusions and suggests future work that can be explored based on the findings and limitations of the master's thesis.

## 7.1 Conclusion

In this master's thesis, the application of a PI controller has been investigated for a linear DC/DC converter. The controller utilized the inductor current error as input to the proportional channel and the capacitor voltage error as input to the integral channel. The primary objective has been to achieve a closed-loop GAS system by employing Lyapunov's method. As a motivation for this thesis' objective, the increasing need for RES was highlighted as an introduction.

Global electricity production from renewable technologies is expected to increase, with the EU aiming to reach 42.5% renewable energy production by 2030 [4]. The integration of variable RES using power converter technology poses challenges to power system stability. Power converters, particularly DC/DC converters, are crucial in managing DC voltage levels in power converter applications. Therefore, the objective of this thesis is the stability analysis of a linear DC/DC converter.

The system's model of the linear DC/DC converter was initially transformed into a pH representation to consider the circuit's energy-conserving capabilities. Subsequently, it was shifted to an incremental form to enable the desired operating point at a non-zero equilibrium. Stability analyses were conducted for both open- and closed-loop systems.

The open-loop analysis revealed that the inductor current was the passive output of the incremental model and, thereby, the normal model. While a conventional choice for the input to the channels of a PI controller, considering PI-PBC, is the error signal of the system's passive output, this thesis aimed to consider a linear DC/DC converter operating in voltage-control mode directly in the inner-loop. Based on this proposal, the stability of the closed-loop system using a PI control around the capacitor voltage was analyzed. However, the system could not be rendered stable by employing a PI control solely with the capacitor voltage, indicated in appendix B. Therefore, a PI controller with the inductor current error signal in the proportional channel and the capacitor voltage error signal in the integral channel was proposed instead.

Following this, the closed-loop stability of the proposed PI controller was analyzed by Lyapunov's method. Given a stabilizing condition as a leakage term, requiring voltage deviations in the system's output, the system was rendered GAS. However, the requirements of the stabilizing term were found to be unacceptable through model simulations conducted with parameters obtained from [18]. The leakage term was eliminated to address the voltage deviations, and a new LFC was sought to render the system GAS.

Subsequently, it was proposed to populate an LFC with unknown values, calculate the function's time derivative, and then select the unknown terms to ensure the resulting expression was negative definite. Unfortunately, finding the unknown values in the LFC for this proposed controller was not possible. However, as the system and controller are linear, the Lyapunov equation was used to calculate a numerical Lyapunov function. This numerical function was fully populated without any zero elements, as opposed to the previous LFC.

Finally, the populated LFC was considered to render the system GAS with the inclusion of the leakage term. The aim was to reduce the stabilizing leakage term and minimize the voltage deviations in the system's output. Increasing the conductance $G$, as demonstrated in section 5.2.2, raised the dissipation value of the system and improved the possibility of proving GAS using the populated LFC. With the new value of $G$, the unknown value in the LFC was calculated, and together these values were utilized to find a new stabilizing condition for the leakage term. Simulation results for this system demonstrated a notable decrease in voltage deviations, effectively eliminating them. However, the increased value of $G$ resulted in high spikes for the control signal and increased losses in the system.

## 7.2 Future Works

Based on the discoveries made in this master's thesis, several avenues for future work become apparent. Additionally, the limitations outlined in section 1.3 present opportunities for further investigation and exploration.

The process of populating the LFC in chapter 5 did not obtain a stability certificate. However, the system was rendered GAS by another numerical Lyapunov function, calculated by the Lyapunov equation. The result from this calculation highlighted the differences between a valid Lyapunov function and the proposed LFC for the system. An interesting result was that the proposed LFC had some zero elements, whereas the numerical Lyapunov function was fully populated. This observation gave room for improvement of the proposed LFC, as seen in section 5.3.2. Continuing the work with this section as a starting point and finding existing values for the constants $\varepsilon$ and $a$ would make the stability certificate more general and, thereby, robust.

Further, the limitations presented initially in this master's thesis have affected the findings. The system has been considered with linear dynamics, which is a simplification of the system as it is more typical for power converters to be considered with non-linear dynamics due to switching characteristics, etc. If the system is considered non-linear instead, control strategies have to be developed to handle these dynamics. However, the findings presented in this thesis are a contribution that gives insight into how the system is affected.

Further, the interconnection between multiple DC/DC converters forms a complex power system. This will address challenges associated with system coupling. Instead, or in addition, integrating RES in a grid-connected or energy storage system with a DC/DC converter. Future research on stability in systems where the DC/DC converter is not standalone.

And lastly, to verify the stability certificate and the results from this thesis, which relied on mathematical and simulation models, work related to experimental validation can be conducted.

# Bibliography


[1] Astrid Sigurdsøn. *Power Electronics Energy Cybernetics for Scalable Stability Certificates: Rethinking Inner Control Loops*. Specialization Project Report in TET4510. Department of Electric Energy, NTNU – Norwegian University of Science and Technology, Dec. 2022.

[2] International Energy Agency. *Renewables 2022*. Paris, 2022. URL: https://www.iea.org/reports/renewables-2022.

[3] United Nations. *The Paris Agreement*. visited on 2023-06-05. 2023. URL: https://unfccc.int/process-and-meetings/the-paris-agreement.

[4] European Union. *Renewable energy target*. visited on 2023-06-05. 2023. URL: https://energy.ec.europa.eu/topics/renewable-energy/renewable-energy-directive-targets-and-rules/renewable-energy-targets_en.

[5] European Environment Agency. *Share of energy consumption from renewable sources in Europe (8th EAP)*. visited on 2023-06-05. 2023. URL: https://www.eea.europa.eu/ims/share-of-energy-consumption-from.

[6] International Renewable Energy Agency. *World Energy Transitions Outlook 2022: 1.5°C Pathway*. visited on 2023-06-05. Abu Dhabi, 2022. URL: /-/media/Files/IRENA/Agency/Publication/2022/Mar/IRENA_World_Energy_Transitions_Outlook_2022.pdf?rev=6ff451981b0%5Cnewline948c6894546661c6658a1.

[7] Julia Matevosyan et al. 'Grid-Forming Inverters: Are They the Key for High Renewable Penetration?' In: *IEEE Power and Energy Magazine* 17.6 (2019), pp. 89–98. DOI: 10.1109/MPE.2019.2933072.

[8] Carlos Collados-Rodriguez et al. 'Stability and operation limits of power systems with high penetration of power electronics'. In: *International Journal of Electrical Power & Energy Systems* 138 (2022), p. 107728. ISSN: 0142-0615. DOI: https://doi.org/10.1016/j.ijepes.2021.107728. URL: https://www.sciencedirect.com/science/article/pii/S0142061521009534.

[9] Angelo Lunardi et al. 'Grid-Connected Power Converters: An Overview of Control Strategies for Renewable Energy'. In: *Energies* 15.11 (2022). ISSN: 1996-1073. DOI: 10.3390/en15114151. URL: https://www.mdpi.com/1996-1073/15/11/4151.

[10] Walter Gil-González, Alejandro Garces and Oscar Danilo Montoya. 'Current PI Control for PV Systems in DC Microgrids: A PBC Design'. In: *2019 IEEE Workshop on Power Electronics and Power Quality Applications (PEPQA)*. 2019, pp. 1–5. DOI: 10.1109/PEPQA.2019.8851555.

[11] Michael Hernandez-Gomez et al. 'Adaptive PI Stabilization of Switched Power Converters'. In: *IEEE Transactions on Control Systems Technology* 18.3 (2010), pp. 688–698. DOI: 10.1109/TCST.2009.2023669.

[12] Hassan K. Khalil. *Nonlinear Systems*. 3rd. Pearson Education Limited, 2015.

[13] Antonio Loría and Henk Nijmeijer. *Passivity based control*. EOLSS publishers, 2004.

[14] A. van der Schaft and D. Jeltsema. 'Port-Hamiltonian Systems Theory: An introductory Overview'. In: *Foundations and Trends in Systems and Control* 1.2-3 (2014), pp. 173–378.

[15] C. R. Johnson. 'Positive Definite Matrices'. In: *The American Mathematical Monthly* 77.3 (1970), pp. 259–264. ISSN: 00029890, 19300972. URL: http://www.jstor.org/stable/2317709 (visited on 14/12/2022).

[16] Jean Gallier. 'Schur Complements and Applications'. In: *Geometric Methods and Applications: For Computer Science and Engineering*. New York, NY: Springer New York, 2011, pp. 431–437. ISBN: 978-1-4419-9961-0. DOI: 10.1007/978-1-4419-9961-0_16. URL: https://doi.org/10.1007/978-1-4419-9961-0_16.

[17] Bayu Jayawardhana et al. 'Passivity of nonlinear incremental systems: Application to PI stabilization of nonlinear RLC circuits'. In: *Systems & Control Letters* 56.9 (2007), pp. 618–622. ISSN: 0167-6911. DOI: https://doi.org/10.1016/j.sysconle.2007.03.011. URL: https://www.sciencedirect.com/science/article/pii/S0167691107000497.

[18] Gerardo Becerra et al. 'A unified hybrid control for DC/DC power converters using port-Hamiltonian formulation'. In: *IECON 2017 - 43rd Annual Conference of the IEEE Industrial Electronics Society*. 2017, pp. 4851–4856. DOI: 10.1109/IECON.2017.8216837.

# Appendix A

# Preliminaries

This chapter contains relevant matrice definitions obtained in [1], and the proof showing that the system and incremental models are equivalent.

## A.1 Matrix Defintions

The necessary matrix definitions for the system are given in this section.

Firstly, the state vector of the pH system:

$$x = \begin{bmatrix} \Phi_L \\ q_C \end{bmatrix}$$

The controller vectors are given as $g$, current control, and $\hat{g}$, voltage control:

$$g = \begin{bmatrix} 1 \\ 0 \end{bmatrix} \quad \text{and} \quad \hat{g} = \begin{bmatrix} 0 \\ 1 \end{bmatrix}$$

The transformation matrix Q, which is symmetric and positive definite:

$$Q := \begin{bmatrix} \frac{1}{L} & 0 \\ 0 & \frac{1}{C} \end{bmatrix}$$

The system's open-loop passive output:

$$y = g^\top Q x = i_L$$

Voltage control is introduced in the integral channel of the PI controller:

$$y_2 = \hat{g}^\top Q x = v_C$$

The skew-symmetric matrix $\mathcal{J}_o$ for the pH form.

$$\mathcal{J}_o := \begin{bmatrix} 0 & -1 \\ 1 & 0 \end{bmatrix}$$

The skew-symmetric property means that $\mathcal{J}_o = -\mathcal{J}_o^\top$:

$$-\mathcal{J}_o^\top = -\left(\begin{bmatrix} 0 & -1 \\ 1 & 0 \end{bmatrix}\right)^\top = -\begin{bmatrix} 0 & 1 \\ -1 & 0 \end{bmatrix} = \begin{bmatrix} 0 & -1 \\ 1 & 0 \end{bmatrix} = \mathcal{J}_o$$

The dissipation matrix $\mathcal{R}$ is positive definite and symmetric.

$$\mathcal{R} := \begin{bmatrix} R & 0 \\ 0 & G \end{bmatrix}$$

The system matrix is given as $\mathcal{F}_o := \mathcal{J}_o - \mathcal{R}$.

$$\mathcal{F}_o = \begin{bmatrix} -R & -1 \\ 1 & -G \end{bmatrix}$$

The Hamiltonian of the system, $\mathcal{H}$:

$$\mathcal{H} := \frac{1}{2} x^\top Q x = \frac{1}{2} \left( \frac{\Phi_L^2}{L} + \frac{q_C^2}{C} \right)$$

and its gradient, $\nabla \mathcal{H}$:

$$\nabla \mathcal{H} = \frac{\partial}{\partial x} \mathcal{H} = \frac{\partial}{\partial x} \left( \frac{1}{2} x^\top Q x \right) = \frac{1}{2} \cdot 2 Q x = Q x = \begin{bmatrix} i_L \\ v_C \end{bmatrix}$$

## A.2 Proof Incremental Model

The mathematical proof that the system and the incremental models are equivalent, in addition to the calculations conducted to obtain the incremental modes.

The definition of the incremental model: $\tilde{(\cdot)} = (\cdot) - \bar{(\cdot)}$. This is used to shows that the dynamics of the incremental model and of the original model of the system are equivalent:

$$\dot{\tilde{x}} = \frac{d}{dt}\tilde{x} = \frac{d}{dt}(x - \bar{x}) = \dot{x} - \dot{\bar{x}} = \dot{x}$$

$\dot{\bar{x}}$ is the dynamics for the system in steady-state, which are zero. Since $\dot{\tilde{x}} = \dot{x}$, it is evident that the representations are equivalent.

**The Hamiltonian $\mathcal{H}$**

$$\mathcal{H}(\tilde{x}) = \mathcal{H}(x) - \mathcal{H}(\bar{x}) = \frac{1}{2}x^\top Qx - \frac{1}{2}\bar{x}^\top Q\bar{x} = \frac{1}{2}(x - \bar{x})^\top Q(x - \bar{x}) = \frac{1}{2}\tilde{x}^\top Q\tilde{x}$$

$$\nabla\mathcal{H}(\tilde{x}) = \frac{\partial}{\partial\tilde{x}}(\mathcal{H}(\tilde{x})) = \frac{\partial}{\partial\tilde{x}}\left(\frac{1}{2}\tilde{x}^\top Q\tilde{x}\right) = Q\tilde{x}$$

**The State Space Model**

$$\begin{aligned}\dot{\tilde{x}} = \dot{x} - \dot{\bar{x}} &= [\mathcal{J}_0 - \mathcal{R}]\nabla\mathcal{H}(x) + gu + E_o - ([\mathcal{J}_0 - \mathcal{R}]\nabla\mathcal{H}(\bar{x}) + g\bar{u} + E_o) \\ &= [\mathcal{J}_0 - \mathcal{R}]\nabla\mathcal{H}(\tilde{x}) + g\tilde{u}\end{aligned}$$

The system's output:

$$\tilde{y} = y - \bar{y} = gQ(x - \bar{x}) = gQ\tilde{x}$$

and when the output is changed to voltage:

$$\tilde{y}_2 = \hat{g}Q(x - \bar{x}) = \hat{g}Q\tilde{x}$$

**The Controller State $x_c$ and the Controller $u$**

When the controller state is brought to equilibrium, i.e., $\dot{\bar{x}}_c = 0$ since its steady state, there is no change.

$$\dot{\tilde{x}}_c = \frac{d}{dt}(x_c - \bar{x}_c) = (\dot{x}_c - \dot{\bar{x}}_c) = \dot{x}_c$$

The incremental form of the controller is easily obtained by subtracting the equilibrium points:

$$\tilde{u} = u - \bar{u} = -K_P(y - \bar{y}) + K_I(x_c - \bar{x}_c) = -K_P\tilde{y} + K_I\tilde{x}_c$$

# Appendix B

# PI control around the capacitor voltage

This appendix considers a PI controller using the capacitor voltage error as input to the proportional and integral channels. By use of LFC $\mathcal{V}_2$, it was not possible to prove a stable system, and based on an eigenvalue analysis conducted for the system, this PI controller is not advantageous for stability.

Some of the material in this appendix's chapter is obtained from section 4.2.2 in [1].

The system's state equations given in incremental form:

$$\begin{cases} \dot{\tilde{x}} = (\mathcal{J}_o - \mathcal{R})Q\tilde{x} + g\tilde{u} \\ \dot{\tilde{x}}_c = -\hat{g}^\top Q\tilde{x} - DK_I\tilde{x}_c \end{cases}$$

And the controller in incremental from:

$$\tilde{u}_2 = -Kp\tilde{y}_2 + K_I\tilde{x}_c = -\hat{g}^\top Q\tilde{x} + K_I\tilde{x}_c$$

The LFC $\mathcal{V}_2$ is used, the same as in section 3.2.2.

$$\mathcal{V}_2(\tilde{x}, \tilde{x}_c) = \frac{1}{2}\tilde{x}^\top Q\tilde{x} + \frac{1}{2}\tilde{x}_c^\top K_I\tilde{x}_c$$

The time-derivative of $\mathcal{V}_2$ is calculated.

$$\begin{aligned} \dot{\mathcal{V}}_2 &= -\tilde{x}^\top Q\mathcal{R}Q\tilde{x} - \tilde{x}^\top QgK_P\hat{g}^\top Q\tilde{x} + \tilde{x}^\top QgK_I\tilde{x}_c - \tilde{x}_cK_Ig^\top Q\tilde{x} - \tilde{x}_c^\top K_IDK_I\tilde{x}_c \\ &= \begin{bmatrix} \tilde{x}^\top Q & \tilde{x}_c^\top K_I \end{bmatrix}^\top \begin{bmatrix} \mathcal{R} + \hat{K}_P & \frac{1}{2}(\hat{g} - g) \\ \frac{1}{2}(\hat{g} - g)^\top & D \end{bmatrix} \begin{bmatrix} Q\tilde{x} \\ K_I\tilde{x}_c \end{bmatrix} \end{aligned}$$

Using $\hat{K}_P := gK_P\hat{g}^\top$.

To determine if $\dot{\mathcal{V}}_2$ is negative definite, the matrix's Schur complement must be calculated. A condition for this is that is that $\mathcal{R} + \hat{K}_P > 0$ and invertible.

$\mathcal{R} > 0$ because it is a diagonal matrix with positive eigenvalues. The positive definiteness of $\hat{K}_P$ needs to be checked as well. The symmetric part of $\hat{K}_P$ is obtained using (2.5.1).

$$\begin{aligned}\hat{K}_{P,sym} &= \frac{1}{2}\left(gK_P\hat{g}^\top + \hat{g}K_Pg^\top\right)\\ &= \frac{1}{2}\left(\begin{bmatrix}K_P\\0\end{bmatrix}\begin{bmatrix}0 & 1\end{bmatrix} + \begin{bmatrix}0\\K_P\end{bmatrix}\begin{bmatrix}1 & 0\end{bmatrix}\right)\\ &= \frac{1}{2}\begin{bmatrix}0 & K_P\\K_P & 0\end{bmatrix}\\ &= \frac{K_P}{2}\begin{bmatrix}0 & 1\\1 & 0\end{bmatrix}\end{aligned}$$

$\hat{K}_{P,sym}$ is a off-diagonal matrix with positive values. The eigenvalues of $\hat{K}_{P,sym}$ are found through eigenvalue analysis: $\det(\lambda I - \hat{K}_{P,sym}) = 0$.

$$\begin{aligned}\det(\lambda I - \hat{K}_{P,sym}) &= \det\left(\begin{bmatrix}\lambda & 0\\0 & \lambda\end{bmatrix} - \begin{bmatrix}0 & \frac{K_P}{2}\\\frac{K_p}{2} & 0\end{bmatrix}\right)\\ &= \det\left(\begin{bmatrix}\lambda & -\frac{K_P}{2}\\-\frac{K_p}{2} & \lambda\end{bmatrix}\right) = \lambda^2 - \frac{K_P^2}{4}\end{aligned}$$

$$\lambda^2 - \frac{K_P^2}{4} = 0 \Rightarrow \lambda_{1,2} = \pm\frac{K_P}{2}$$

The eigenvalues of $K_{P,sym}$ are positive and negative. Therefore, the sign of the eigenvalues is indeterminant. In $\mathcal{R} + \hat{K}_P$, where $\mathcal{R}$ usually is chosen to be positive but small to minimize losses. So in the case of a negative eigenvalue, $\mathcal{R}$ won't be able to compensate, and $\mathcal{R} + \hat{K}_P < 0$. The analysis shows clearly that complete voltage control is not advantageous for stability. And it is not possible to calculate the Schur complement of the matrix.

# Appendix C

# Droop Control

In this chapter, the concept of droop control is introduced. This control is more suitable to apply when more than one power converter is considered. However, the scope of the master's thesis is limited to considering one converter. Therefore, calculations are only done for a single converter without considering other components, and this chapter is included as a part of the appendix.

## C.1 The Concept of Droop

A system is considered stable if the output signal follows the reference quickly without too many oscillations. A PI controller is used with a feedback mechanism such that the error between the measured output signal and a desired setpoint is removed. As stated in the theory chapter, the integral part of the controller integrates the deviation between the signal to reduce it. Due to this, and the fact that it is easy to understand and implement, the PI controller is very popular and common.

In a power system with RES, in addition to conventional power production, converters using PI controllers are connected together. An issue with a network of converters using PI controllers is stability. The technology of a PI controller only works as intended for a network if the desired setpoints (references) of the units are identical. In a power system, the different converters will have different desired setpoints depending on the RES and calculations for the load flows, which will make the value similar but not identical.

Because of the integral effect in the PI controller, each controller has a strict goal of eliminating the deviation between response and reference. When the different units have different references, the controllers will work against each other to make each error zero. As a consequence, the system would be unregulated, which would also lead to instability.

Instead of just using the conventional PI controller, a scheme using both the PI controller and droop control could be implemented. Droop control is commonly used when regulating conventional power production. For instance, in hydropower production, to regulate the stability of the turbines' speed according to the frequency value, i.e., with droop for power and frequency. For converter technology, the controller is not implemented in the same way, but the concept remains the same, with droop for a V-I graph. Droop control is not as strict in regulating the error as it accepts a small error to exist. The droop characteristic lets the converters share the voltage reference.

## C.2 Calcuations for Droop

The combination of PI controller and droop control is considered for system (3.1.4) and the normal PI controller (3.1.6). The controller state $\dot{x}_c$ is set to voltage regulation, such that the controller regulates both current and voltage.

The system's setup includes a load flow, and one of the reference values for $i_L$ is calculated in this, while the reference value for $v_C$ is used directly in the controller. Due to this, the equilibrium point value for current $\bar{i}_L \neq i_L^{ref}$ is instead given as $\bar{i}_L = i_L^*$. $i_L^*$ is the output from the load flow and is used as input to the controller. While the voltage, on the other hand, remains $\bar{v}_C = v_C^{ref}$. This is also considered in section 3.2.2.

The droop setting is considered for the linear relationship between voltage and current, which is derived from the state equation of the controller state, $\dot{x}_c$:

$$\dot{x}_c = -\hat{g}^\top Q(x - x^{ref}) = -y_2 \tag{C.2.1}$$

The controller has both current and voltage control and is therefore given as:

$$u = -K_P g^\top Q(x - x^*) + K_I x_c \tag{C.2.2}$$

The steady-state equations of the controls consider equilibrium points $\bar{x}$ instead of normal state $x$. Since the time derivative of an equilibrium point represents the change in the system during a steady state, it is zero, as seen in (C.2.4).

$$\bar{u} = -K_P g^\top Q(\bar{x} - x^*) + K_I \bar{x}_c \tag{C.2.3}$$

$$0 = -\hat{g}^\top Q(\bar{x} - x^{ref}) \tag{C.2.4}$$

As explained previously, for voltage control $\bar{x} = x^{ref}$ and for current control $\bar{x} = x^*$. When obtaining the incremental model of the controller $u$, these have to be considered differently:

$$\begin{aligned}
\tilde{u} &= u - \bar{u} \\
&= -K_P g^\top Q(x - x^*) + K_I x_c - \left(-K_P g^\top Q(\bar{x} - x^*) + K_I \bar{x}_c\right) \\
&= -K_P g^\top Q(x - \bar{x}) + K_I (x_c - \bar{x}_c) \\
&= -K_P g^\top Q\tilde{x} + K_I \tilde{x}_c
\end{aligned}$$

When the controller is shifted to the incremental form, $x^*$ is eliminated from the equations. And the incremental form for the controller is the same as used previously in (3.1.8). In the controller state, voltage control is considered, and there is no need to consider $x^*$, which makes the calculations to incremental form the same as in the appendix A.2.

$$\dot{\tilde{x}}_c = -\hat{g}^\top Q\tilde{x} \tag{C.2.5}$$

The incremental equations for the controller $\tilde{u}$ and $\dot{\tilde{x}}_c$ obtained in this chapter is the same as were considered in section 3.2.1. It is unnecessary to conduct the stability analysis once more, and the same result from section 3.2.1 can be applied in this case. The stability was proved, given a constant leakage in the voltage output. Equation (C.2.5) has to include a constant leakage term.

In chapter 4, simulations were conducted to verify the proof of the system where the leakage is included.

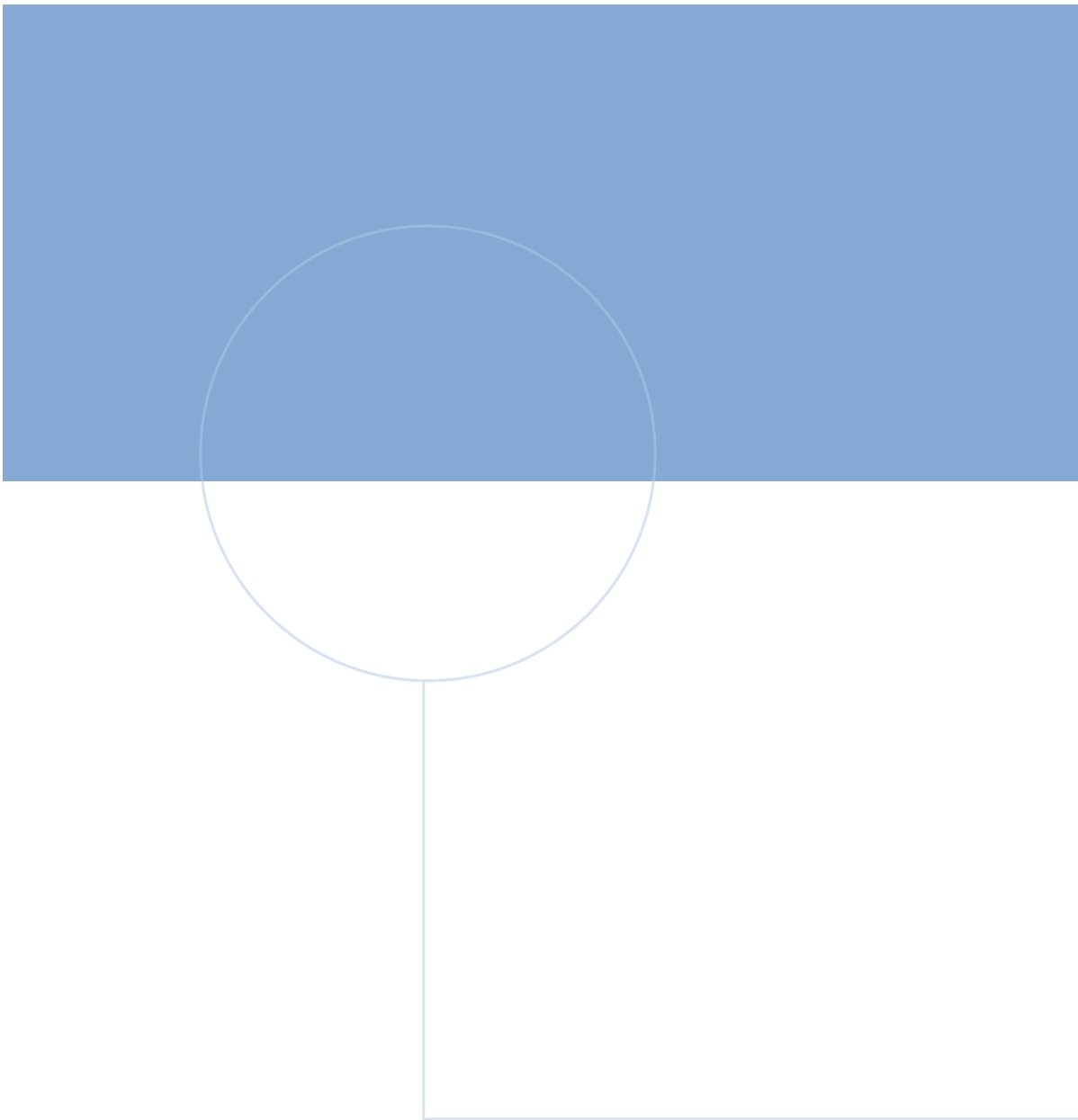

NTNU

Norwegian University of
Science and Technology